การสลายด้วยแสงของฟิล์มยางธรรมชาติสำหรับการประยุกต์ด้านแก๊สธรรมชาติ

วรรณนิภา อมาตยกุล

PHOTO-DEGRADATION OF NATURAL RUBBER FILMS
FOR NATURAL GAS APPLICATION

WANNIPHA AMATYAKUL

A Dissertation Submitted in Partial Fulfillment of the Requirements
for the Degree of Doctor of Philosophy Program in Chemical Technology
Department of Chemical Technology
Faculty of Science
Chulalongkorn University
Academic year 2006
Copyright of Chulalongkorn University
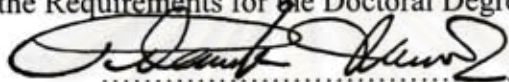
Thesis Title   PHOTO-DEGRADATION OF NATURAL RUBBER
                    FILMS FOR NATURAL GAS APPLICATION
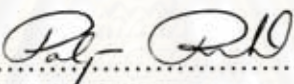
By   Wannipha Amatyakul

Filed of Study   Chemical Technology
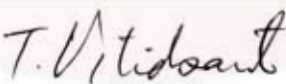
Thesis Advisor   Pienpak Tasakorn, Ph.D.

Accepted by the Faculty of Science, Chulalongkorn University in Partial
Fulfillment of the Requirements for the Doctoral Degree

.... Dean of the Faculty of Science

(Professor Piamsak Menasveta, Ph.D.)
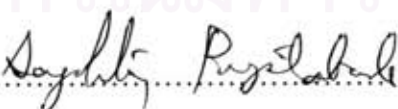
THESIS COMMITTEE

.... Chairman

(Professor Pattarapan Prasassarakich, Ph.D.)

.... Thesis Advisor

(Pienpak Tasakorn, Ph.D.)

.... Member

(Associate Professor Tharapong Vitidsant, Ph.D.)

.... Member

(Associate Professor Somkiat Ngamprasertsith, Ph.D.)

.... Member

(Assistant Professor Sangobtip Pongstabodee, Ph.D.)

.... Member

(Polpatr Pruksananont, Ph.D.)

วรรณนิภา อมาตยกุล : การสลายด้วยแสงของฟิล์มยางธรรมชาติสำหรับการประยุกต์ด้านแก๊สธรรมชาติ. (PHOTO-DEGRADATION OF NATURAL RUBBER FILMS FOR NATURAL GAS APPLICATION) อ. ที่ปรึกษา : อ. ดร. เพียรพรรค ทัศคร, 93 หน้า.

ยางธรรมชาติสามารถทำให้สลายตัวได้ด้วยปัจจัยหลายประการ เช่น ความร้อน แรงกล ปฏิกิริยาเคมี และแสง โดยแสงเป็นปัจจัยที่น่าสนใจ เนื่องจากแสงสามารถทำให้ยางธรรมชาติสลายตัวได้ภายใต้อุณหภูมิและความดันต่ำ ในงานวิจัยนี้ได้มีการทดลองสลายยางธรรมชาติด้วยแสงเพื่อศึกษาผลของแสง อุณหภูมิ และตัวเร่งปฏิกิริยา ที่มีต่อการลดลงของมวลโมเลกุลของฟิล์มยางธรรมชาติ โดยได้นำฟิล์มยางธรรมชาติที่ผสมและไม่ผสมตัวเร่งปฏิกิริยา อันได้แก่ ไทเทเนียมไดออกไซด์ (Titanium dioxide) และโพแทสเซียมเพอร์ซัลเฟต (Potassium persulfate) ไปฉายแสงจากหลอดไฟปรอทที่ความหนาแน่นแสงและอุณหภูมิต่างๆ หลังจากนั้นนำฟิล์มยางธรรมชาติไปวิเคราะห์หามวลโมเลกุลด้วยวิธีเจลเพอร์มิเอชันโครมาโทกราฟี หรือจีพีซี (Gel permeation chromatography, GPC) แล้วศึกษาการลดลงของมวลโมเลกุล และนำข้อมูลการแจกแจงของมวลโมเลกุลที่ได้จากการวิเคราะห์ด้วยจีพีซี ไปคำนวณหาจำนวนของพันธะคู่ในฟิล์มยางธรรมชาติ สมการทางจลนพลศาสตร์สำหรับปฏิกิริยาลำดับที่หนึ่งที่มีการตัดสายโซ่แบบสุ่มได้นำมาประยุกต์ใช้กับกระบวนการสลายตัวด้วยแสงนี้ และยังมีการศึกษาสมบัติทางกายภาพอื่นๆ ของฟิล์มยางธรรมชาติอีกด้วย

ความรู้พื้นฐานที่ได้นี้ สามารถนำมาพัฒนายางธรรมชาติเพื่อนำไปใช้ในการบรรจุมีเทนไฮเดรต (Methane hydrate) หรือใช้ดูดซับแก๊สเชื้อเพลิง

ภาควิชา............เคมีเทคนิค.............. ลายมือชื่อนิสิต........วรรณนิภา อมาตยกุล........

สาขาวิชา............เคมีเทคนิค.............. ลายมือชื่ออาจารย์ที่ปรึกษา..............

ปีการศึกษา..........2549..................

4573831823   : MAJOR CHEMICAL TECHNOLOGY

KEY WORD: NATURAL RUBBER / PHOTO-DEGRADATION / TITANIUM DIOXIDE / POTASSIUM PERSULFATE / GPC

WANNIPHA AMATYAKUL : PHOTO-DEGRADATION OF NATURAL RUBBER FILMS FOR NATURAL GAS APPLICATION.   THESIS ADVISOR : PIENPAK TASAKORN, Ph.D., 93 pp.

Natural rubber (NR) can be degraded depending on various factors such as heat, mechanical force, chemical reaction, and light. Light is an attractive factor because it degrades NR under low temperature and pressure. In this research, the photo-degradation of NR films was carried out to investigate the effects of the light, temperature, and catalysts on the reduction of the weight-average molecular weight (Mw) and the double bonds in the NR films. The NR films, with and without catalysts, titanium dioxide (TiO_2), and potassium persulfate ($K_2S_2O_8$), were exposed to light from a mercury light bulb at different light densities and temperature. After exposure, the Mw of the NR films was analyzed using the gel permeation chromatography (GPC) method. The reduction of Mw was studied, and the Mw distribution information from the GPC was used to calculate the number of double bonds in the NR films. A kinetic model for the 1st order reaction with random scission has been applied to this photo-degradation process. Some other physical properties of the NR films were also investigated.

From this fundamental knowledge obtained, NR can probably be developed for a containment of methane hydrate, or for adsorption of gaseous fuels.

Department.....Chemical Technology.... Student's signature................................

Field of study...Chemical Technology... Advisor's signature................................

Academic year............2006...........

Acknowledgement

Contents

Chapter I

Introduction

Natural rubber (NR) is mainly composed of hydrocarbon substance, which can be cast into films that are usable for many purposes such as wrapping, decorative coating, protective covering, light screening or blocking, separating, and producing new types of materials or compounds.

The rate of energy consumption gets higher nowadays and tends to be much higher in the future. The amount of fuels, which are important energy resources, for example: oil, and coals, has been reduced rapidly due to the growth of energy consumption and tends to be exhausted in the near future. The renewable energy such as sunlight, biodiesel, and biomass, becomes an alternative choice because its resources can be produced naturally in a short period of time. Another attractive resource of energy is gas hydrates, for example: methane hydrate from natural gas. Methane hydrate is a crystalline solid consisting of a methane molecule surrounded by a cage of water molecules. It looks like ice flakes or ice cream and occurs abundantly in nature, but still inconvenient to be utilized. In the future, fuels may be present in various forms, for example: methane hydrate. Because methane hydrate appears as a solid, which cannot flow, so it is inconvenient to be used as a fuel. If it is covered with a film to make it a small round particle here called "energy particle", it will be transported, stored, and utilized conveniently. The application of NR films in this manner is essential for the development of fuels conversion from gas to solid state. NR is a hydrocarbon substance obtained from the rubber trees that can be grown in our life cycle. Its molecular structure is composed of active C=C, so it can be introduced into various kinds of reactions in order to improve or change its properties. According to the above reasons, it is possible to produce films from the NR in order to cover or store fuels, and that the films can also be burned together with fuels.

Another interesting point is that NR is a good candidate for replacing plastic, which creates disposal problems because it is difficult to be degraded naturally, but NR is degraded quite easily. On the other hand, if NR is used to replace plastic, it should have some resistant properties for some instance. Therefore, before moving on to the application step, the fundamental knowledge should be studied.

NR can be degraded depending on various factors such as heat, mechanical force, chemical reaction, and light. Light is a very interesting factor because it can cause the NR to degrade under low temperature and pressure. When the NR is exposed to light, the energy transferred from the light will activate the NR into the excited state. In this state, there can be several kinds of reactions occurring, which change the properties of the NR or produce new types of compounds. The photo-degradation is an attractive process to be used to improve or change the properties of NR because it can be held at low temperature and pressure. Further more, we can find the rate of photo-degradation of NR films in order to identify its lifetime or to release the fuels at the desired rate by photo-degrading the films. So it is very interesting to study the photo-degradation process of NR films to gain some fundamental knowledge in order to modify the rubber or to improve its properties, and also to make the products more valuable.

The objectives of this work are
1) To study the effect of light, catalyst, peptizer, and retardant on the breaking of double bonds in the natural rubber films.
2) To find the rate of change of natural rubber molecular weight in the photo-degradation process.

The most interesting factor in this work is light, which can degrade the NR films at low temperature and pressure. Other factors of interest are the chemicals or materials that can accelerate or retard the rate of degradation or change the properties of the NR films, which are catalyst, peptizer, and retardant. The catalyst used in this work was titanium dioxide (TiO_2) (anatase), which is reported that it can accelerate the rate of photo-degradation of some polymers and organic materials. The peptizer used is potassium persulfate ($K_2S_2O_8$), which is an oxidant. TiO_2 (anatase) is also used as retardants.

In order to accomplish what are stated above, the experiments were set up.
1) Investigation of the effect of the factors on the photo-degradation of natural rubber films

Two-level factorial experimental design was used to screen the factors having an effect on the experiments. The factors of interest in this work are light density,

exposure time, and types and concentrations of catalyst, peptizer, and retardant. This design was used to confirm that these factors really had an effect on the photo-degradation of NR films and that there was nothing uncommon in the experimental system.

The NR films were exposed to light for a period of time and were collected at various intervals. The controlled and collected samples were kept in a dry cool dark place.

2) Investigation of the rate of molecular weight change

If the films are to be used to store something, their lifetime should be identified. The properties of the NR films, especially the weight-average molecular weight (Mw), which relates to the size of the rubber molecules, can represent the characteristic of the films. If the rate of Mw change is known, the lifetime of the films is predictable. On the other hand, the rate of change can be controlled if the relationships between the Mw change of the films and the factors affecting it are recognized.

The NR films with different concentration of catalyst, peptizer, and retardant were exposed to light of different intensities for a period of time, and were collected at various intervals to find the rate of Mw change. The experiments were carried out at different temperatures, 25 and 80°C, because the films are expected to be used under low temperature.

The relationships between the properties of the NR films, especially Mw, and the factors: light density, types and concentration of the chemicals, temperature, were examined in the terms of rate of change.

3) Characterization of the natural rubber films

3.1) Molecular weight and molecular weight distribution

The Gel Permeation Chromatography (GPC) was used to investigate the Mw of the NR films, which relates to the size of the rubber molecules. The Mw distribution was also considered because many properties of a polymer show a strong dependence on Mw distribution, as well as on the Mw.

3.2) Viscosity of the rubber solution

The viscosity of a polymer solution relates to the size and shape of the dissolved polymer.

3.3) Tensile strength

The tensile strength of a polymer represents its resistance to elongation or breaking when stretching forces are applied to it. This is one of the important characteristics of the films that are used for wrapping or storing things.

3.4) Gas permeability

The permeability of the rubber films to gases such as methane, and moisture must be taken into account when choosing a film for packaging of fuels like natural gas hydrates.

3.5) Functional groups

The functional groups present in the natural films are characterized by using the Fourier Transform Infrared Spectroscopy (FTIR). This is one of the methods leading to understanding of the photo-degradation mechanisms.

3.6) The surface characteristic

The microscope was used to examine the surface of the NR films before and after the exposure.

3.7) Moisture content

Moisture content in the NR films must be determined because it has an effect on the degradation process.

4) Characterization of titanium dioxide

4.1) Particle size distribution

The particle size distribution of TiO_2 was measured by using the Particle Size Laser Analyzer. The particle size of the fillers may have an effect on the catalytic or retarding properties and also on the mechanical properties of the rubber films.

5) Simulation of the utilization of the natural rubber films at low temperature

The NR films were used to store the ice at the temperature below 0°C to test the probability of the films utilization under the real condition.

Chapter II

Theory, Literature Review and Hypothesis

2.1.   Natural rubber (Barlow, 1993: 9-25)

The definition of the term *rubber* is given in ASTM D 1566-05a, Standard Terminology Relating to Rubber (ASTM D 1566-05a: 9):

> **rubber,** *n*—a material that is capable of recovering from large deformations quickly and forcibly, and can be, or already is, modified to a state in which it is essentially insoluble (but can swell) in boiling solvent, such as benzene, methyl ethyl ketone, or ethanol-toluene azeotrope.
>
> DISCUSSION—A rubber in its modified state, free of diluents, retracts within 1 min to less than 1.5 times its original length after being stretched at room temperature (18 to 29°C) to twice its length and held for 1 min before release.

Technical definitions of rubber are of interest not only to compounders. Customs officers, for example, require a precise definition of rubber to ensure that the appropriate import duty, if any, is collected.

NR was the first rubber and was unique until the development of polysulfide rubber in about 1927. NR supplies about one-third of the world demand for elastomers and is the standard by which others are judged. It was Charles Goodyear and Thomas Hancock's experiments with NR, sulfur, and heat that led to the discovery of vulcanization, representing the birth, as it were, of compounding.

2.1.1. Properties

Chemically, NR is *cis*-1, 4-polyisoprene. A linear, long-chain polymer with repeating units (C_5H_8), it has a density of 0.93 at 20°C. Intensive plant breeding has produced a wide range of clonal types whose Mooney viscosity (when freshly coagulated) can vary from slightly below 50 to over 90. Mooney viscosity is a common test for toughness of a rubber; the higher the value, the more resistant to deformation. Paralleling this Mooney range is a very wide range of molecular weights. Since, however, rubber in commerce is a blend of rubbers from various clones, the spread is less. It has been estimated that a random blend would have a

weight-average molecular weight of perhaps 2 million and a number average molecular weight of 0.5 million.
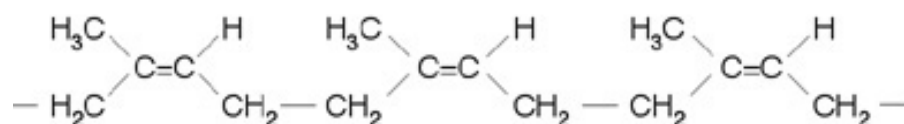
Figure 2.1 *cis*-1, 4-polyisoprene.

Due to the blending mentioned above, the Mooney viscosity for commercial rubbers is approximately 60 when first made. However, crosslinking of aldehyde groups on the rubber molecule causes the Mooney viscosity to rise in storage and in transit to the consumer, so that rubber received in a plant may be between 75 and 100.

Table 2.1   Typical analysis of natural rubber.

Component	%
Moisture	0.6
Acetone extract	2.9
Protein (calculated from nitrogen)	2.8
Ash	0.4
Rubber hydrocarbon	93.3
	100.0

Because of its regular structure, NR crystallizes when stretched, or when stored at temperatures below 20°C. The rate of crystallization varies with the temperature and also with the type of rubber, grades like pale crepe rubber (light colored rubbers often used in pharmaceutical products) freezing faster than smoked sheet. Since frozen rubber is almost rock-hard and practically impossible to mix, large users often have "hot rooms" to thaw frozen rubber they might receive. Temperatures are usually 50-70°C, and the bales are separated because of the low thermal

conductivity of the rubber, 0.00032 cal/sec/cm^2/°C. Frozen rubber is not a common problem but it does occur (e.g. when rubber is stored or transported in unheated sheds or railway cars subject to low temperatures for days or even weeks).

In a typical NR sample (Table 2.1), the acetone extract contains various sterols, esters, and fatty acids. Certain NR antioxidants are also found in the acetone extract. The proteins and fatty acids are highly useful as vulcanizing activators.

2.1.2. Production

Commercially all NR is derived from the species *Hevea brasiliensis*. This tree grows most readily in a band within 5° of the equator, in places where the annual rainfall exceeds 80 in./year, the temperature is 25-35°C, and low altitudes prevail. More than 80% of NR comes from Southeast Asia: production is about equal in Malaysia and Indonesia; Thailand accounts for much of the remainder in this area. *H. brasiliensis* is grown on estates and by small holders. By intensive plant breeding, tree productivity has been greatly increased. In the 40-year period 1930-1970 yield jumped from 1,000 to more than 3,000 lb/acre/year for the best stock.

The milky, rubber-bearing fluid in the tree is called latex and is obtained by process called tapping. A cut, about 22° to the horizontal, is made into the bark of the tree cutting the latex vessels nearby. The latex exuding from the cut follows a vertical channel at the lower end of the cut into a small ceramic or glass cup. In the cutting process a small portion of the bark is excised. The latex flows for about 4 hrs, and auto-coagulation is prevented by placing a small amount of liquid ammonia in the cup. At the end of this prime flow period the latex is collected by the tapper and bulked in tanks. Usually 2 days later the auto-coagulated material (cup lump) is removed from the cup and saved, a fresh cut is made beneath the previous one, ammonia is added, and the cycle repeated. Perhaps 80% of the flow is collected as liquid latex, up to 20% as cup lump, and very minor amounts collected as coagulum on the tree cut (tree lace) and at the foot of the tree (earth scrap). Latex fresh from the tree is called whole-field latex and will have 30-40% total solids by weight. The lower grades of NR are prepared from cup lump, partially dried small holders' rubber, tree lace and earth scrap, after appropriate cleaning.

The essence of dry NR production is that whole-field latex, stabilized against coagulation by ammonia or other materials, is collected in bulk, screened to remove

foreign matter, diluted, and the rubber coagulated with acid. The coagulum, a white spongy mass, is squeezed between contrarotating rollers to remove much of the water and serum and then dried to a moisture content of less than 1% by heat. Somewhat strangely, the squeezing operation uses a copious supply of iron-free water to wash the coagulum on the roll mills. The purpose is to wash out all traces of serum from the coagulum, the liquid that remains when the rubber is coagulated from the latex. Iron-free water is used to prevent oxidative deterioration of the rubber in storage. Variations in the feed mix, coagulation, and drying methods result in the different grades.

Despite acceptance of newer technically specified rubbers, a significant portion of the rubber used is called ribbed smoked sheet, usually abbreviated to RSS followed by the grade number. Ribbed smoked sheet is made from whole-field latex. It is diluted to about 15% solids and then coagulated with dilute formic acid. Coagulation usually takes place overnight. The coagulum is then passed through successive two-roll mills, which squeeze much of the water out. The last pair of rollers has ribs that impart a ribbed appearance to the sheet and increase the surface area, to expedite drying. The sheets from the last mill are draped on poles, supported by a framework, which is wheeled into the smokehouse. Here the rubber is dried, very much like clothes on a line, for 2-4 days at 40-55°C. Losing its water, the white sheet turns a yellow-brown color in the smoke house and has a distinctive smoky smell. The rubber now has less than 1% moisture and is more fungus-resistant due to fungicides in the wood smoke.

For the lightest colored rubber products, a light-colored, premium priced, NR called pale crepe may be used. This product calls for the use of clones having low yellow pigment content (mostly carotene) and higher resistance to discoloration by oxidation.

Technically specified natural rubbers were developed in the 1960s to make NR more attractive in view of the competition from synthetic rubber. The production process is not much different from that for smoked sheet up to and including the coagulation stage. However, upon coagulation the sheet, after roll mills have pressed most of the water out of it and it is in the form of a continuous narrow blanket, is mechanically torn into crumbs. These are then dried in sieved-bottom trays by passing them through oil-fired air circulating tunnel driers at 100°C. Such a process can and

does use such feedstock as cup lump and unsmoked partially dried sheet rubber. The dried crumb rubber is then compressed into $33\frac{1}{3}$-kg bales, which have a standard size of $66 \times 33 \times 18$ cm, wrapped in thin polyethylene film, and packed into crates containing 1 metric ton. Although installations for making technically specified block rubber require much more capital than traditional methods, they speed up the process, allow much more quality control, and package the product in a commercial way. The polyethylene film prevents adhesion between bales, keeps water out, and yet disperses easily when the rubber is mixed in the consumer's factory because of its low melting point.

Before the introduction of technically specified rubber, autocoagulated rubbers such as cup lump, tree lace, and earth scrap were washed, carefully blended, and milled till a relatively uniform product was obtained and dried. Some of these materials, called brown crepes, are still available, although a large and increasing percentage of feed material for these types now goes to the lower quality grades of technically specified rubbers.

2.1.3. Grades and grading

All types of NR that are not modified (such as oil-extended NR) or technically specified rubbers (TSRs) are considered to be international grades. The current grades in this category are listed and specified in the booklet *International Standards of Quality and Packing for Natural Rubber Grades*, commonly called the Green Book from the color of its cover and obtainable in the United States from the Rubber Manufacturers Association. Also, master samples of the grades are kept at various organizations for reference and arbitration purposes.

Grade designations usually use color or how the rubber was made; typical grade descriptions are pale crepe #2, ribbed smoked sheet #1, and thin brown crepe #3. The main disadvantage of this system is that grading is done on visual aspects. Almost exclusively, the darker the rubber, the lower the grade. RSS #4, for example, is considerably darker than RSS #1. Other grading criteria, such as the presence or absence of rust, bubbles, mold, and wet spots, are subjective in nature. Perhaps the most valid assumption is that the darker the rubber, the more dirt it contains.

In the 1960s Malaysia led in developing a grading scheme that was more sophisticated and useful to consumers. A major criticism of NR was the large and

varying dirt content. The cornerstone of the new system was grading according to dirt content, measured in hundredths of 1%. For example, Standard Malaysian Rubber (SMR) #5 is a rubber whose dirt content does not exceed 0.05%. Dirt is considered to be the residue on a 45-μm sieve after a rubber sample has been dissolved in an appropriate solvent, washed through the sieve, and dried.

The specification has other parameters, including source material for the grade, ash and nitrogen content, volatile matter, plasticity retention index (PRI), and initial plasticity. Acceptance of these standards was vigorous, and other producing countries followed suit. Letter abbreviations identify the rubber source: SMR was rubber from Malaysia, SIR indicated Indonesian production, SSR Singapore, and so on.

Again following the Malaysian lead, Standards organizations such as the American Society for testing and Materials (ASTM) And the International Standards Organization (ISO) have evolved specifications of their own.

2.1.4. Modifications of natural rubber

NR has been modified in many ways since the establishment of a continuous supply of plantation rubber. Some of these modifications, such as chlorinated rubber, have passed their peak of acceptance as other materials supplanted them. Several others, however, can be very useful in compounding. In some instances the supply will be available before adopting one for productions runs.

Deproteinized rubber (DPNR) is a useful rubber when low water absorption is wanted, vulcanizates with low creep are needed, or more than ordinary reproducibility is required. Normally NR has between 0.25 and 0.50% nitrogen as protein; deproteinized rubber only about 0.07%. One tradeoff occurs here: since protein matter in the rubber accelerates cure, deproteinized rubber required more acceleration.

Deproteinized rubber is made by treating NR latex with a bio-enzyme, which hydrolyzed the proteins present into water-soluble forms. A protease like *Bacillus subtilis* is used at about 0.3 part per hundred of rubber by weight. The enzymolysis process may take a minimum of 24 hr. When complete, the latex is diluted to 3% total solids and coagulated by adding a mixture of phosphoric and sulfuric acids. The coagulated rubber is then pressed free of most of the water, crumbed, dried, and baled.

DPNR is viscosity stabilized at 60 Mooney. The heavy dilution of the latex helps reduce the dirt and ash contents, and respective values of 0.006 and 0.06% are not unusual. Properly compounded, a black loaded stock (say 30 parts of SRF black) would give a stress relaxation rate of 2%/decade. Other vaulcanizate properties would be a Shore A hardness of 50, elongation of 550%, and tensile strength of 3700 psi.

Oil-extended NR (OENR) is also made in the Far East, especially Malaysia. Three ways have been used to make this type of rubber: (1) co-coagulation of latex with an oil emulsion, (2) Banbury mixing of the oil and rubber, and (3) allowing the rubber to absorb the oil in pans until almost all is absorbed, then milling to incorporate the remaining oil and produce a sheet. More recently, rubber and oil have been mixed using an extruder. Properties of the finished product do not differ significantly irrespective of the method used.

There is no strict limit on how much oil can be incorporated into NR; it is a question of how oily a product can be handled. An arbitrary limit might be set as 65 parts of oil per 100 of rubber. Both aromatic and naphthenic oils are used.

Oil-extended NR masterbatches are used where high black and oil contents are wanted in a NR stock or blends with NR. Incorporation of large amounts of oil is easier if some portion of the oil is already in the rubber. Another advantage is that the masterbatches are freeze-resistant. Oil-extended NR masterbatch has not been used much in North America but has enjoyed some popularity in Eastern Europe and Japan.

Latex is not the only form of liquid rubber; depolymerized rubber is also available in certain areas. In the United States it is made by Hardman Inc. of Belleville, NJ, under the trade name DPR. Production details are proprietary. The product look somewhat like molasses and comes in two grades, a low viscosity grade (45,000-75,000 CP/sec at 100°C) and a high viscosity grade (175,000-400,000 CP). Viscosity measurements are made in a Brookfield viscometer. These rubbers can be compounded in a split batch compound to give self-curing compounds as well as by using a conventional cure system vulcanized by heat. These rubbers fill a niche for applications in which conventionally prepared rubber would be unsatisfactory. For example, they make excellent flexible molds to release waxes, gypsums, and ceramics easily with excellent surface reproduction and dimensional stability. Other uses

include binders in grinding wheels, dispersants, and automotive sealants. DPR compounds are not recommended for outdoor exposure.

A comparatively new modification of NR produced in commercial quantities is epoxidized NR (ENR). The rubber molecule is partially epoxidized, with the epoxy groups randomly distributed along the molecular chain. Commercially two grades were developed, identified by the extent of the modification: 25 mol % epoxidized and 50 mol % epoxidized. With epoxidation, a segment of the molecular chain looks like this:
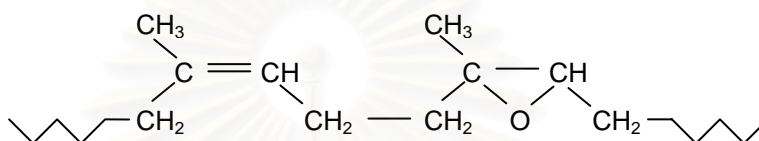
These products, formed by the addition of oxidizing agents on latex, were developed by the Malaysian Rubber Producers Research Association (MRPRA) In conjunction with the Rubber Research Institute of Malaysia. The developers used the designations ENR 25 and ENR 50; commercial brands may carry other names. Kumpulan Guthrie Berhad in Malaysia, for example, have described the properties of their Epoxyprene brands in a series of studies.

The properties of these rubbers are so unique they might be considered to be new elastomers. Although the Mooney viscosity at 70-100 parallels much NR, the specific gravity increases significantly, as does the glass transition temperature, as epoxidation is increased. For the 25 and 50% epoxidized materials, one commercial producer lists specific gravities of 0.97 and 1.03 and glass transition temperatures of -45 and -20°C, respectively.

Of interest to compounders are the following advantages the epoxidized polymers have over NR:

1) Improved oil resistance – ENR 50 is similar to chloroprene rubber.
2) Low gas permeability – ENR is similar to butyl rubber.
3) Because of the polarity induced by the epoxidation, these rubbers are compatible with polyvinyl chloride, which suggests their use in adhesives.
4) With epoxidized rubber and precipitated silica as the reinforcer, of the reinforcement properties obtained are very similar to those of NR and carbon black. This is done without the use of expensive coupling agents.

In processing and compounding, epoxidized rubbers differ from conventional rubbers. Little if any premastication is required. It is easy to overmix the polymer. Vulcanization systems commonly used with unsaturated polymers can be selected, but semiefficient or efficient systems give better aging. Thermal degradation of epoxidized rubber occurs differently than NR and it is customary to add 2-5 parts of calcium stearate to combat it. Protective systems against ozone attack are generally higher than with unmodified NR, and levels of 3.5-6.0 parts per hundred of rubber are not uncommon.

2.2. Polymer degradation (Kelen, 1972: 1-9)

Polymer degradation is the collective name given to various processes, which degrade polymers, i.e., deteriorate their properties or ruin their outward appearance.

Generally speaking, polymer degradation is a harmful process, which is to be avoided or prevented. The operation that can be undertaken to inhibit or to retard degradation is called polymer stabilization. In order to do this suitably, with maximum efficiency, the mechanism of polymer degradation must be understood, the factors and stresses causing it must be identified, and the factors that affect polymer stability must be known.

Sometimes polymer degradation may be useful. Depolymerization leading to high purity monomers may be exploited for practical production of such materials. Another important field in which degradation is desirable is the destruction of polymeric waste materials.

2.2.1. Polymer life phases and degradation

Degradation may happen during every phase of a polymer's life, i.e., during its synthesis, processing, and use. Even after the polymer has fulfilled its intended purpose, its degradation may still be and important problem.

Depending on polymerization conditions, during polymer synthesis depolymerization may take place. Depolymerization is the inverse of polymerization, namely, a stepwise separation of the monomers from the growing chain end. Polymerization is possible only below the equilibrium temperature of the system, the so-called ceiling temperature. From a practical point of view, it is important that the eventual fate of the polymeric material is often decided during its synthesis.

Depending on the polymerization technology, varying amounts of "weak sites" may be built into the polymer which will later occasion its deterioration. For example, the presence of tertiary chlorines in PVC resulting from branch formation during polymerization may reduce PVC stability. During synthesis, various contaminants such as catalyzer residues or other polymerization additives may enter the polymer. The presence of impurities may be very decisive with respect to polymer life span. The amount of additives used during PVC polymerization techniques increases in the sequence block-suspension-emulsion; the stability of the polymer decreases in the same sequence.

During processing, the material is subjected to very high thermal and mechanical stress. These drastic stresses may initiate a variety of polymer degradation processes leading to a deterioration of properties even during processing. On the other hand, the damaging of the material may result in the introduction of various defects in the polymer which will work as degradation sources during its subsequent service life. For example, in the presence of oxygen traces during processing, carbonyl groups can be formed in polyolefins; these will later absorb UV light during outdoor applications and thus will function as built-in sensitizers for photo-degradation processes. In PVC, a small amount of HCl may be eliminated from the polymer during processing. This alone does not influence the properties very much, but the resultant double bonds and the allyl-activated chlorines joined with them are very dangerous sources of PVC degradation.

Because of the dual nature of degradation during processing, i.e., deterioration and introduction of defects as potential sources of deterioration, it is very important to add stabilizers to the polymer before processing. This is necessary not only in cases in which processing supplies finished products, but also during intermediate (e.g., granule) production.

The best known appearance of polymer degradation is connected with the use of these materials. Some kinds of polymers degradation, such as the outdoor aging of PVC roofs or the stiffening and discoloration of badly composed vinyl handbags, etc., are well known. The scale of polymer applications is, however, very broad; consequently, the stability requirements are highly diverse. In most cases there is a demand for a long service life; sometimes only a predicted (usually short) lifetime is required. Some types of mulch foils for horticultural applications may be completely

destroyed after their useful life of several weeks or months. Underground cables for telecommunication or heavy current applications are, however, expected to last several decades. In both of these examples, the polymers are in contact with the soil and the same types of bacteria probably attack them; the biodegradability of the polymers employed should thus be very different.

The problem of waste disposal is increasing with the use of increasing amounts of plastic materials. Organized recovery presently exists only in the case of production wastes inside polymer factories. In domestic garbage there is and every-increasing portion of plastic wastes, the destruction of which requires expensive equipment. During the burning of one pound of PVC, approximately 160 liters of HCl are evolved, which is very undesirable because of air pollution. Protection of the environment requires improved packaging materials which are "self-destructing", i.e., which will be degraded very rapidly when exposed to the effects of sunlight, humidity, and – finally – soil bacteria.

2.2.2. Factors and stresses causing degradation

Macromolecules are composed of monomeric units which are joined by chemical bond to each other. The monomeric units contain chemical bonds which either are in the main chain of the macromolecule or connect various atoms or side groups to it. Side groups, if they are present, contain additional chemical bonds. All of these bonds may be reaction sites in polymer degradation, and various energy sources may be effective in supplying the energy necessary to break the bonds. The bond energies are manifold and depend not only on the kind of atoms connected by the bond but also on the chemical and physical characteristics surrounding the bond. The dissociation energies of chemical bonds in common polymers range from about 65 kcal/mol (C–Cl) to 108 kcal/mol (C–F) with carbon-carbon bonds in the middle (75-85 kcal/mol). The most important types of energy that cause the degradation are heat, mechanical energy, and radiation. Thermal and mechanical degradation of polymers may occur during thermomechanical processing. An extreme case of heat damage is burning; the flammability and combustion behavior of polymers are very important in many applications. A typical example of pure mechanical destruction of a polymeric material is grinding, although the evolved heat may play a role even in this case. The most common form of radiant energy which causes degradation is that of the UV

component of sunlight; the energy of a photon with $\lambda = 300$ is about 95 kcal/mol, which is higher than most bond dissociation energies in polymers. In special applications, e.g., polymers used in x-ray laboratories in hospitals or in plastic parts for aerospace applications, nuclear radiation may cause degradation.

Not only is the role of temperature important when the heat necessary for bond dissociation is supplied by thermal motion of the atoms, it can also activate various chemical and biological processes. Reactions of polymers with oxygen and moisture, generally present in various applications, are very important in polymer degradation. Ozone degradation of elastomers is of the utmost importance in the rubber industry. Recently, the stability of the polymers in the presence of pollutant gases such as sulfur dioxide and nitrogen dioxide has aroused interest. However, the factors generally are not separated; various combinations of damaging components (e.g., heat, mechanical stress, moisture, and oxygen) may initiate very complex processes. The stresses may be sudden and of short duration (e.g., a hammer blow), but they may also act for a much extended time period. The behavior of the same polymer under impact and fatigue conditions may differ to a great extent; this is also true when other types of stress, not just mechanical, are involved.

As a result of degradation processes, initiated and completed by the above factors or their combination, the internal properties as well as the external appearance of the polymers may change. Chain scission and cross-linking lead to a change of Mw distribution; oxidation and other chemical reactions, in the side chains too, cause changes in chemical composition result in discoloration, etc. These primary alterations in the polymer usually cause the deterioration of mechanical and other technically important properties; as a result, the material loses its value and becomes a useless waste. It is, therefore, of great practical importance to know the factors affecting polymer stability.

2.2.3. Factors affecting polymer stability

The chemical structure of the polymer is of primary importance in respect to its stability. The chemical composition (i.e., what kinds of chemical bonds in what sort of arrangement) is in itself a decisive factor. Bond energies between the same atoms belong. A few selected data are included in Table 2.2.

Tertiary and allylic bonds are usually weaker than primary or secondary ones. In polymers consisting only of primary and secondary carbon atoms (e.g., PVC), the presence of such bonds is undesirable because these form weak sites which are very easy to attack. Processes leading to these bonds during polymerization (e.g., PVC branching or dehydrochlorination) are to be avoided.

Table 2.2 Bond dissociation energies of various single bonds.

Bond Broken A─B	Bond Dissociation Energies (kcal/mol)	Bond Broken A─B	Bond Dissociation Energies (kcal/mol)
C_2H_5─H	99	C_6H_5─CH_3	94
n-C_3H_7─H	98	$C_6H_5CH_2$─CH_3	72
t-C_4H_9─H	91	CH_3─Cl	84
CH_2=$CHCH_2$─H	82	C_2H_5─Cl	81
C_6H_5─H	103	CH_2=$CHCH_2$─Cl	65
$C_6H_5CH_2$─H	83	CH_3─F	108
C_2H_5─CH_3	83	C_2H_5─F	106
n-C_3H_7─CH_3	83	HO─OH	51
t-C_4H_9─CH_3	81	t-C_4H_9O─OH	36

The dissociation energies of the various bonds in the polymer may determine the course of degradation: the process always begins with the scission of the weakest available bond or with an attack at this site, and the first step usually determines the further direction of the process. Other components of the chemical structure, such as steric factors, stability of the intermediates, or the possibility of their resonance stabilization, may also have great influence on degradation. Such factors may even change the value of the bond dissociation energies.

Table 2.3 shows the effect of steric factors and resonance stabilization on bond dissociation energies of some CH_3─R bonds. Some comonomeric units incorporated in the copolymers may influence stability. Such units usually modify the application properties of the polymer, for example, the T_g or mechanical strength; they can, however, also improve the stability. Thus, the incorporation of a few percent of

dioxolane units into polyformaldehyde greatly reduces its depolymerization because the dioxolane units inhibit the unzipping of formaldehyde units.

Table 2.3 Bond dissociation energies of some CH_3–R bonds.

–R	Bond Dissociation Energies (kcal/mol)
–CH_3	88.4
–C_2H_5	84.5
–n-C_3H_7	84.9
–n-C_4H_9	84.7
–i-C_3H_7	83.8
–t-C_4H_9	80.5
–CH_2–$CH=CH_2$	73.6
–$CH(CH_3)$–$CH=CH_2$	72.3
–CH_2–C_6H_5	71.9
–$CH(CH_3)$–C_6H_5	68.7
–$C(CH_3)_2$–C_6H_5	65.7
–$CH=CH_2$	93.7
–C_6H_5	94
–CH_2–OH	82.1
–CH_2–C(O)–CH_3	79
–CH_2–CN	77.1

The presence of some comonomeric units, like the presence of certain additives or polymer blend components which are not chemically bonded to the polymer (although added in order to improve its properties), may decrease stability. For example, the rubber component of high impact polystyrene usually contains unsaturated bonds which are sources of various degradation reactions. High impact polystyrene products are improved materials from the viewpoint of their improved mechanical properties, but they are more sensitive to light or oxidation than polystyrene itself. An increasingly utilized method of improving stability is the chemical modification of polymers. Elimination of weak sites or substitution of labile groups by stable ones via grafting onto the polymer may be very effective and useful

especially when the substituents simultaneously improve other properties. Alkylation of the weak sites in PVC may result in internal plasticization of the material.

The tacticity of the polymer plays an important role in the degradation behavior. Atactic and isotactic polypropylene have very different oxidative stability (the isotactic one is much more stable). Syndiotactic PVC prepared at low temperatures has increased stability compared to the ordinary material produced at about 50°C. It is, however, very difficult to separate the effect of tacticity from that of the morphology of the material because a change in tacticity is usually connected with a change of morphology.

Physical and morphological factors may also influence polymer stability. It is well known that oxidation is always initiated in the amorphous phase of semi-crystalline polymers and the propagation of the oxidation into the crystalline phase is a result of the destruction of the crystalline order. Thus, crystallinity is an important characteristic of the polymer from the viewpoint of stability.

The morphology of the material is decisive from the point of view of diffusion conditions. A compact material is usually more stable against oxidation because the diffusion of oxygen into the product is more difficult than with a material of loose structure. On the other hand, the facile diffusion of HCl evolved from PVC with a loose morphology reduces the autocatalytic character of the degradation which may lead to a catastrophic destruction in the case of compact and dense material.

Similar to the internal chemical stresses already mentioned (weak sites, etc.), the internal mechanical stresses which are left in the material or introduced by finishing operations are very dangerous. Such stresses may serve not only as sources of later mechanical deterioration but also as initiators of, or assistants to, various chemical attacks. This is especially true in cases of stresses with long duration (the so-called stress corrosion of polymers).

The role of contaminants is quite obvious and has already been mentioned in connection with the synthesis of polymers. It is obvious that some additives intentionally present in the material, such as plasticizers or lubricants, influence the stability of the composite, especially if the oxidizability and biodegradability of such systems are higher than those of the polymer components. Once radicals are formed in the additive, they attack the polymer and vice versa; i.e., composites are sometimes less stable than their components. In special cases, additives are intentionally used to

promote degradation of the composites (e.g., photosensitizers or plasticizers) which are specific culture media for bacteria in some rural and horticultural applications. On the other hand, additives may also stabilize the polymer: the use of antioxidants, photostabilizers, etc.

2.2.4. Types of polymer degradation

There are various schemes to classify polymer degradation. Because of its complexity, with regard to both the causes and the response of the polymer, classification is usually performed on the basis on the dominating features. One of the most frequent classifications has been based on the main factors responsible for degradation:

> thermal, thermo-oxidative, photo, photo-oxidative, mechanical, hydrolytic, chemical, and biological degradation; degradation by high energy radiation pyrolysis and oxidative pyrolysis; etc.

Another possible classification is based on the main processes taking place as dominating events during degradation:

> random chain scission, depolymerization, cross-linking, side group elimination, substitution, reactions of side groups among themselves, etc.

The type of degradation that is of interest in this work is photo-degradation, which will be discussed later.

2.2.5. Photo-degradation

Photo-degradation can be divided into several types of processes.

2.2.5.1.   Photo-physical processes

The physical processes involved in photo-degradation include absorption of light by the material, electronic excitation of the molecules, and deactivation by radiative or radiationless energy transitions, or by energy transfer to some acceptor. When the lifetime of the excited state is sufficiently long, the species can participate in various chemical transformations.

2.2.5.2.   Photo-chemical processes

The chemical processes of photo-degradation include isomerization, dissociation, and decomposition of a molecule as a direct consequence of its photo-

physical excitation, as well as those nonunimolecular chemical reactions which are facilitated by the absorbed energy. Obviously, a photochemical reaction can take place only during the lifetime of the excited state; such a reaction must compete with the physical modes of deactivation.

2.2.5.3. Photo-oxidation

Photo-oxidation is degradation involving oxygen, often atmospheric oxygen in practice. Many polymer degradations proceed via free radicals which often result from polymer reaction with oxygen or on to which oxygen readily adds, since it is itself a free radical. Polymer photo-oxidation is very similar to thermal oxidation of polymers. Significant differences exist with respect to the photo-chemical decomposition of the hydroperoxide and carbonyl groups, as well as with regard to the initiation reaction. The formation of polymer radicals

$$RH \xrightarrow{hv} R\bullet + H\bullet \qquad\qquad (1)$$

by scission of a C-H bond is a possible consequence of UV irradiation. The probability of reaction (1) is higher than that of the direct reaction between molecular oxygen and a polymer, although the probability of the latter reaction may be increased due to UV excitation.

2.2.5.4. Sensitized Photo-degradation

The ever-increasing amount of plastic used for disposable packaging material and their potential for causing permanent pollution of the environment have prompted workers to seek methods of producing polymers with controlled service life. After having finished its useful function, e.g., as a container for milk or as a sandwich bag, the plastic becomes a waste material; it is desirable that this waste decomposes with the aid of sunlight, humidity, and bacteria as rapidly as possible. A photo-sensitizer causes rapid degradation of the polymer to low Mw compounds, which are small enough to be decomposed by microorganisms. Thus, the complete deterioration of plastic wastes and the control of service life of plastics are rather complex procedures.

A photo-sensitizer usually has a high absorption coefficient for UV light; the excited compound either decomposes into free radicals and initiates degradation or oxidation of the polymer, or it transfers the excitation energy to the polymer (or to oxygen). A good sensitizer should be easily admixed with the polymer and must not decompose thermally or in the dark.

There have been many research works devoted to photo-degradation of polymer in both aspects of how to stabilize and degrade it. Photo-degradation of various kinds of polymers, pure and blended, has been extensively investigated. The decrease in double bonds and the formation of photoproducts are thoroughly reported. Claudie et al. (1989) studied the photo-oxidation of elastomeric materials. The photo-oxidations of various polybutadienes with different compositions have been compared and found to be very similar. Associated hydroperoxides in the allylic position are primarily formed in the photo-oxidation. The IR spectra of irradiated polybutadienes shows absorption bands, which are ascribed to α, β-unsaturated ketones and saturated acids formed later. Photo- and thermo-unstable hydroperoxides are transformed into α, β-unsaturated ketones. The most outstanding feature is related to the decrease in double bonds and the formation of photoproducts, which leads to an invariant state. The decrease of permeability to oxygen during photo-oxidation implies that oxygen could no longer diffuse through the surface layers, so that photo-oxidation consequently stopped.

Claudie and his coworkers (1990) also had another work released, which is quite similar to this work. They studied the photo-oxidation of 1,2-polybutadiene (84% 1,2, 16% 1,4 *cis*) at long wavelengths (λ > 300 nm). They found that radical addition to the 1,2 double bond is the main oxidation pathway. The tertiary macroradical formed is oxidized to tertiary associated hydroperoxide. Associated peroxides are photolyzed to saturated alcohols or to saturated ketones, absorbing at wavelengths longer than 300 nm, and photo-oxidized to saturated acids. Formation of methylene and methyl groups is revealed by IR analysis during irradiation of the film. The rate of photo-oxidation of 1,2-polybutadiene is five times lower than the rate of photo-oxidation of highly 1,4-*trans* and *cis* polybutadiene. During irradiation of 1,2-polybutadiene, competition between cross-linking and chain scission occurs mainly during formation of ketones and Norrish type I reactions.

Another work done by Claudie and his coworkers (1991) is photo-oxidation of polyisoprene. The photo-oxidation, at long wavelengths, of polyisoprenes with different compositions (i.e. with different relative concentrations of 1,4 *cis*, 3,4 and 1,2 groups) has been compared. They found that abstraction of a hydrogen atom in the allylic position is probably the main oxidation pathway of the 1,4 *cis* unit. The tertiary macroradical formed is oxidized to tertiary associated hydroperoxides. Ketonic groups

(α, β unsaturated and saturated) are detected in the IR spectra of photo-oxidized polyisoprenes at 1693 and 1726 cm^{-1}, respectively. Formation of ketonic groups induced β cleavage and numerous chain-scissions. Viscosity and GPC measurements reveal a decrease in the *Mw* during the earliest stages of irradiation. Other photoproducts are detected: the major ones are alcohols together with acids, esters and epoxides. An addition mechanism occurs and competes with chain scission during irradiation. In the case of 1,2 and 3,4 units, radical addition is probably the main oxidation pathway.

Some other polymers, such as polyethylene and polypropylene, were also investigated for their photo-degradation behaviors (Gijsman et al., 1999: 433-441). The rigid polyurethane foams were found to be harmed by the UV light, and let the CFCs trapped inside escape (Christopher and Forciniti, 2001: 3346-3352). The photo-degradation of synthetic and natural polyisoprenes was studied at specific UV radiations (Santos et al., 2005: 34-43). The types and concentration of the photo-products were analyzed by using the FTIR. It was found that the effect of UV radiation on the photo-oxidation of polyisoprenes depends on the wavelength of UV radiation used as well as on the type of isomer and pre-conditions of the synthetic or natural rubber. Reactions at 253 nm irradiation, leading to reticulation, occur preferentially to those leading to chain scission while at 300 and 350 nm irradiation chain scission prevails. In the case of trans-PI a more rigid structure minimizes the diffusion of molecular oxygen through the polymer network avoiding the complete oxidation of the C=C double bonds.

A car tyre sidewall rubber was exposed to the ultraviolet irradiation while under tensile stress. It was found that tensile stress accelerated degradation (Maillo and White, 1999: 277-287). Another work concerning tensile strain and photo-degradation was done by Bhowmick et al. (2002). They investigated the photo-degradation of thermoplastic elastomeric rubber-polyethylene blends. The experiments were taken with laboratory ultraviolet exposures in the unstrained state and under tensile strain. Strained exposure caused reduction of the strain to failure in subsequent tensile tests. The blends were more resistant to degradation than the NR homopolymer. Photo-oxidation rather than ozone degradation was found to be the major cause of breakdown, even with samples held in tension. Moreover, it is a synergistic effect of increased UV radiation with other factors, such as temperature

that would determine the extent of such reduction in service life (Andrady et al., 1998: 96-103).

2.3. <u>Titanium dioxide</u> (Wikipedia, the free encyclopedia, 2002)

Titanium dioxide, also known as titanium(IV) oxide or titania, is the naturally occurring oxide of titanium, chemical formula TiO_2. When used as a pigment, it is called titanium white, Pigment White 6, or CI 77891. It is noteworthy for its wide range of applications, from paint to sunscreen to food coloring.

Titanium dioxide occurs in four forms:

- rutile, a tetragonal mineral usually of prismatic habit, often twinned;
- anatase or octahedrite, a tetragonal mineral of dipyramidal habit;
- brookite, an orthorhombic mineral. Both anatase and brookite are relatively rare minerals;
- Titanium dioxide (B) or $TiO_2(B)$, a monoclinic mineral.

Titanium dioxide occurrences in nature are never pure; it is found with contaminant metals such as iron. The oxides can be mined and serve as a source for commercial titanium. The metal can also be mined from other minerals such as ilmenite or leucoxene ores, or one of the purest forms, rutile beach sand.

As a pigment of high refringence, titanium dioxide is the most widely used white pigment because of its brightness and very high refractive index (n=2.4), in which it is surpassed only by a few other materials. When deposited as a thin film, its refractive index and color make it an excellent reflective optical coating for dielectric mirrors and some gemstones, for example "mystic fire topaz". TiO_2 is also an effective opacifier in powder form, where it is employed as a pigment to provide whiteness and opacity to products such as paints, coatings, plastics, papers, inks, foods, and most toothpastes. Used as a white food coloring, it has E number E171. In cosmetic and skin care products, titanium dioxide is used both as a pigment and a thickener. It is also used as a tattoo pigment and styptic pencils. This pigment is used extensively in plastics and other applications for its UV resistant properties where it acts as a UV reflector. In ceramic glazes, titanium dioxide acts as an opacifier and seeds crystal formation. In almost every sunscreen with a physical blocker, titanium dioxide is found both because of its refractive index and its resistance to discoloration under ultraviolet light. This advantage enhances its stability and ability to protect the

skin from ultraviolet light. For example, in the photo-degradation of polypropylene, addition of TiO_2 pigment causes a strong reduction in molecular degradation, presumably because it blocks UV penetration and limit photo-degradation to a narrow zone at the surface (Turton and White, 2001: 559-568).

Titanium dioxide, particularly in the anatase form, is a photocatalyst under ultraviolet light. Recently it has been found that titanium dioxide, when spiked with nitrogen ions, is also a photocatalyst under visible light. The strong oxidative potential of the positive holes oxidizes water to create hydroxyl radicals. It can also oxidize oxygen or organic materials directly. Titanium dioxide is thus added to paints, cements, windows, tiles, or other products for sterilizing, deodorizing and anti-fouling properties and is also used as a hydrolysis catalyst. It is also used in the Graetzel cell, a type of chemical solar cell.

Titanium dioxide has potential for use in energy production: as a photocatalyst, it can carry out hydrolysis, i.e., break water into hydrogen and oxygen. Were the hydrogen collected, it could be used as a fuel. The efficiency of this process can be greatly improved by doping the oxide with carbon, as described in "Carbon-doped titanium dioxide is an effective photocatalyst".

As TiO_2 is exposed to UV light, it becomes increasingly hydrophilic; thus, it can be used for anti-fogging coatings or self-cleaning windows. TiO_2 incorporated into outdoor building materials can substantially reduce concentrations of airborne pollutants such as volatile organic compounds and nitrogen oxides.

All the extensive knowledge that was gained during the development of semiconductor photoelectrochemistry during the 1970 and 1980s has greatly assisted the development of photocalalysis (Fujishima et al., 2000: 1-21). In particular, it turned out that TiO_2 is excellent for photocatalytically breaking down organic compounds. For example, if one puts catalytically active TiO_2 powder into a shallow pool of polluted water and allows it to be illuminated with sunlight, the water will gradually become purified.

One of the most important aspects of environmental photocatalysis is the availability of a material such as titanium dioxide, which is close to being an ideal photocatalyst in several aspects. For example, it is relatively inexpensive, highly stable chemically, and the photogenerated holes are highly oxidizing. In addition, photogenerated electrons are reducing enough to produce superoxide from dioxygen.

Catalysts have been introduced into photo-degradation of polymers. TiO_2 is one of the photo-catalysts mostly used in many investigations of photo-degradation of organic materials, such as the photocatalytic decomposition of sodium dodecylbenzene sulfonate surfactant (Zhang et al., 2003: 13-24) and the photocatalytic degradation of metolachlor (Sakkas et al., 2004: 195-205). Further more, titanium dioxide was also modified with silver in order to enhance the photocatalytic efficiency in which it was found to decompose the organic pollutant three-times faster than the pure titanium dioxide (Arabatzis et al., 2003: 187-201).

As well as of organic materials, the photocatalytic degradation of polymers was studied thoroughly. In the solid-phase photocatalytic degradation of PVC-TiO_2 polymer composites, it was found that the photocatalytic degradation localized on the TiO_2–PVC interface and grew cavities around particles while the direct photolytic centers were uniformly distributed in the PVC matrix (Cho and Choi, 2001: 221-228). In some works, it is claimed that TiO_2 particles can absorb UV light ($\lambda < 387$ nm) to create mobile electrons (e^-), and holes (h^+) in the conduction band and valence band, respectively (Shang et al., 2003a: 4494-4499). Adsorbed oxygen molecules can capture electrons, and produce, O, and O^- species. At the same time, photo-generated holes can be trapped by hydroxyl ions, or water adsorbed on the surface, producing hydroxyl radicals, $\bullet OH$, which play important roles in photo-catalytic reactions, as displayed in the following equations.

$$TiO_2 \xrightarrow{\;h\upsilon\;} TiO_2(e^- + h^+) \tag{2.1}$$

$$O_{2\,ads} + e^- \rightarrow O^-_{2\,ads} \tag{2.2}$$

$$O_{2\,ads} \rightarrow 2O_{ads} \tag{2.3}$$

$$O_{ads} + e^- \rightarrow O^-_{ads} \tag{2.4}$$

$$OH^- + h^+ \rightarrow \bullet OH \tag{2.5}$$

$$H_2O_{ads} + h^+ \rightarrow \bullet OH + H^+ \tag{2.6}$$

In the rubber industry, the chemical peptizers are widely used to reduce the viscosity of natural rubber instead of using only mechanical mastication (Hensel et al., 2004: 95-98). The effect of chemical peptizers is very good even in small dosages as 0.1-0.2 phr, but they also produce a lot of short chain material which results in poorer

dynamic properties (Menting et al., 2004: 48-51). Some literature has reported the use of potassium persulfate ($K_2S_2O_8$), which is a peptizer, in the photo-degradation process (Kubota et al., 2001: 223-227). It is revealed that photo-irradiation promotes surface oxidation of polyethylene film with $K_2S_2O_8$. It is interesting to introduce chemical peptizers into photo-degradation process of natural rubber which they can probably be used as photocatalysts.

2.4.   Kinetic model (Tanford, 1961: 611-614)

The dissociation of polymer molecules into smaller units is known as degradation. This process, like its opposite, polymerization, may be studied kinetically, and such kinetic studies are particularly useful for naturally occurring macromolecules the polymerization of which cannot be studied in the laboratory. For natural macromolecules we cannot hope to obtain from *in vitro* experiments any information on the method of synthesis in the living system, but we can by studying the degradation decide whether our ideas concerning the way monomer units are joined in the polymer molecule are reasonable.

In the simplest situation all bonds of a macromolecular chain are equally susceptible to rupture, and bonds are broken at a rate proportional to the number of intact bonds remaining. This situation would be expected to prevail, for instance, in the degradation of simple condensation polymers. When these polymers are synthesized the formation of bonds appears to occur in a completely random fashion. When they are degraded the rupture of bonds might likewise be expected to be a random process.

The other extreme of degradation can be exemplified by the enzymatic hydrolysis of proteins. In this case each bond between monomer units is a peptide bond, but the side chains extending from any pair of adjacent monomer units are in general different. The ability of an enzyme to attack the peptide bond will in general depend on the nature of these side chains, so that bond rupture will occur preferentially at certain specific spots along the polypeptide chains of protein molecules.

The simplest possible degradation occurs when we begin with a polymer sample formed by random polymerization and subject it to non-specific degradation, so that bonds are broken at random. Suitable polymers might be condensation

polymers, polymerization of which leads to the statistical molecular weight distribution, or addition polymers which, owing to chain transfer, have the same kind of distribution. Degradation of such polymers can be carried out by hydrolysis or alcoholysis (polyesters and polyamides) or by heating or ozone treatment (addition polymers).

Degradation is often followed experimentally by determination of the molecular weight as a function of time, using light scattering or viscosity as a measure of molecular weight. These techniques can be applied only as long as the molecular weight remains large; i.e., in terms of the number of bonds broken, these methods involve a study of the initial stages of the reaction only. From the derivation, an equation for a 1st order rate reaction is obtained as followed.

$$\frac{1}{Mw} = \frac{1}{Mw_0} + \frac{kt}{2M_0} \qquad (2.7)$$

This equation is used for random depolymerization, where

k	=	1st order rate constant,
t	=	degradation time,
Mw	=	weight-average molecular weight at time t,
Mw_0	=	weight-average molecular weight at $t = 0$, and
M_0	=	molecular weight of the monomer unit.

Some literature has used this equation for the random depolymerization, for example, enzymatic degradation of oat β-glucan (Roubroeks et al., 2001: 275-285). A linear curve was obtained when plotted 1/Mw versus hydrolysis time at the first stage of degradation, which exhibited a pseudo 1st order reaction.

2.5.   Proposed method of calculation of double bonds in the natural rubber films

Many researchers have studied the photo-degradation of polymers. One of their interests is the reduction of double bonds in the polymer chain, which is mostly studied by using IR technique. Adam et al. (1991) investigated photo-oxidation of polyisoprene, and analyzed the products of degradation by using IR spectroscopy. As well as Adam, Santos et al. (2005) pursued photo-degradation of synthetic and natural

polyisoprenes at specific UV radiations. From the plots of the formation of photoproducts and consumption of double bonds versus time in Adam and Santos's works, the patterns of the reduction of double bonds in polyisoprenes are similar in that they do not decrease immediately, but they keep quite constant for some time before decreasing at a fast rate. The rate of reduction then becomes slower, and the reduction finally stops.

In this work, the number of double bonds was calculated from the information of GPC distribution curve to see if it is possible to predict the number of double bonds from the known *Mw*. This will be useful in the case that if the *Mw* data has already been obtained from GPC analysis, and we want to know the information about the double bonds reduction, instead of using instrumental analysis again such as FTIR, we can then calculate the number of double bonds immediately from the known data. To make the calculation become easier, it is supposed here that the degradation process only occurs at the double bonds, and the NR contains only polyisoprene chains. The calculation is started by slicing the GPC distribution curve into 100 pieces, in which each piece represents the weight (*Wt*) of NR having one *Mw*, and is done on the basis of 1 kg of NR. So the area under the curve is the weight fraction of 1 kg of NR. The number of molecules (*n*) of NR in each fraction (*x*) at time *t* is then calculated from

$$ n_{x,t} \;=\; \frac{Wt_{x,t}}{Mw_{x,t}} \times 6.02 \times 10^{23} \qquad (2.8) $$

where $Wt_{x,t}$ is the *Wt* of NR in each fraction at time *t*, and $Mw_{x,t}$ is the *Mw* of NR in each fraction at time *t*. The total number of molecules or the molecular chains of NR at time *t* ($n_{total,t}$) is the summation of the number of molecules of NR in each fraction.

$$ n_{total,t} \;=\; \sum_{x=1}^{100} n_{x,t} \qquad (2.9) $$

Imagine that we have one molecular chain of NR. If we break one double bond in the chain, we will get two chains of NR. If we break 9 double bonds in the chain, we will get 10 chains of NR. We can see that the total chains obtained are more than the broken bonds in the number of 1. From this idea, if $n_{total,t}$ is the number of molecules or the molecular chains obtained from breaking the double bonds, then it has a relationship with the broken double bonds at time *t* (B_t) as followed.

$$ B_t = n_{total,t} - 1 \qquad (2.10) $$

Since the number of molecules is very large compared to 1, so equation (10) becomes

$$B_t = n_{total,t} \qquad (2.11)$$

That is, the number of broken bonds is equal to the number of molecules.

Suppose that an ideal NR has only one long polyisoprene chain. Each isoprene unit contains one double bond. Therefore, the number of double bonds in the ideal NR (D_{ideal}) is equal to the number of isoprene unit, which can be calculated as followed:

$$D_{ideal} = \frac{Wt_{NR}}{M_0} \times 6.02 \times 10^{23} \qquad (2.12)$$

where Wt_{NR} is the weight of NR, and M_0 is the Mw of an isoprene unit.

Finally, we can obtain the number of double bonds in NR at time t (D_t) from

$$D_t = D_{ideal} - B_t \qquad (2.13)$$

2.6. Solution viscosity (Allcock et al., 2003: 452-468)

2.6.1. Solution viscosity and molecular size

In the early days of polymer chemistry, it was observed that even a low concentration of a dissolved polymer markedly increases the viscosity of a solution relative to that of the pure solvent. This increase in viscosity is caused principally by the unusual size and shape of the dissolved polymer and by the nature of solutions of high polymers.

Most polymer molecules are best described not as long thin rods but as random statistical coils. In dilute solution these coils are free from entanglement with other coils but are completely solvated, which means they have taken up as much solvent as they can hold. Thus, the smallest entities of solute in a polymer solution are not the actual polymer molecules but rather the large, irregularly shaped "particles" made up of polymer coils and large numbers of absorbed solvent molecules. As far as motion through the solution is concerned, the polymer coil and absorbed solvent form a single entity which is actually much heavier than the polymer molecule itself. In many respects, each polymer "particle" resembles a completely saturated sponge. On the basis of the size of these solute "particles", polymer solutions are correctly classified as *colloidal dispersions*. Each colloidal particle is a solvent-filled polymer coil; hence, they are sometimes called *molecular colloids*.

For a long time it has been known that the large particles in colloidal solutions or dispersions tend to impede the flow adjacent layers of liquid when the liquid is subjected to shearing force. In other words, the viscosity of the liquid is increased relative to that of the pure solvent by the presence of a colloidal or polymeric solute. As long ago, it was shown that in the case of spherical colloid particles, the relative viscosity is given by the expression

$$\eta_r = \frac{\eta}{\eta_0} = 1 + 2.5\phi_2 \qquad (2.14)$$

where η_r is the relative viscosity, η the viscosity of the solution, η_0 the viscosity of the pure solvent, and ϕ_2 the volume fraction of the colloidal particle. According to (2.14), as the overall size or volume of the colloidal particle (i.e., polymer molecule plus imbibed solvent) increases, so do the volume fraction ϕ_2 and the relative viscosity. Because the molecular weight of a polymer molecule also increases with size, it is possible to relate the increase in solution viscosity to the molecular weight.

2.6.2. Measurement of viscosity

2.6.2.1. Principles

According to Newton's law of viscous flow, the frictional force, F, which resists the flow of any two adjacent layers of liquid, is given by

$$F = \eta A \frac{d\upsilon}{dx} \qquad (2.15)$$

where A is the area of contact of the layers, $d\upsilon/dx$ the velocity gradient between them, and the proportionality constant, η, is called the coefficient of viscosity or, simply, the viscosity. The unit of viscosity is the poise (i.e., 1 poise = 1 g-cm^{-1}-s^{-1}).

When and external driving force is applied to overcome the frictional resistance and cause the liquid to flow uniformly through a tube, the rate of flow is given by Poiseuille's law,

$$\frac{dV}{dt} = \frac{\pi R^4 \Delta P}{8\eta L} \qquad (2.16)$$

In (2.16), dV/dt is the volume of liquid that flows through the tube per unit time; R and L are the radius and length of the tube, respectively; and ΔP is the difference in external pressure between the ends of the tube. In practice, measurements are usually carried out in viscometer tubes in which the capillary is in a vertical position and the

driving force is simply the weight of the liquid itself. Therefore, the pressure difference, ΔP, which is the driving force per unit area, is given by

$$\Delta P = h\rho g \tag{2.17}$$

where h is the average height of the liquid during measurement, ρ the density, and g the acceleration due to gravity. Substitution of (2.17) into (2.16), along with the assumption of a constant flow rate, yields equation (2.18) for the viscosity.

$$\eta = \frac{\pi R^4 h g \rho t}{8LV} \tag{2.18}$$

The applicability of (2.18) demands that the flow be "Newtonian" or "viscous." This will be true provided that a dimensionless quantity, called the Reynolds number, is less than 1000. In terms of the variables of (2.18) this condition is given by

$$\frac{2V\rho}{\pi R \eta t} < 1000 \tag{2.19}$$

and is readily satisfied for the apparatus and liquids usually used for measurements of viscosities of polymer solutions. However, in addition to the requirements of viscous flow, the derivation of (2.18) relies on the following assumptions:

1) All of the potential energy of the driving force is expended in overcoming the frictional resistance. This is not strictly true, since some energy must be expended to accelerate the liquid in the tube. When this "kinetic-energy correction" is made, equation (2.18) becomes

$$\eta = \frac{\pi R^4 h g \rho t}{8LV} - \frac{\rho V}{8\pi L t} \tag{2.20}$$

For measurements of the *absolute* viscosity, this correction term can amount to 10 to 15% but, for measurements of the *relative* viscosities of interest in polymer chemistry (see equation 2.14), the error introduced by the use of (2.18) rather than (2.20) is usually less than 2%.

2) The second assumption is that the velocity of the liquid at the walls of the capillary is zero (i.e., there is no "slippage" of the liquid along the walls). This assumption is usually valid for liquids that "wet" the capillary walls. In any event, viscosities of polymer solutions are measured relative to the pure solvent and, unless the presence of small concentrations of polymer

markedly affects the surface tension of the solvent, such capillary effects may be neglected.

Although expressions (2.18) and (2.20) are usually used, in practice it is not necessary to make precise measurements of the viscometer tube dimensions. Thus, if (2.20) is written in terms of the *kinematic viscosity, η/ρ*, we have

$$\frac{\eta}{\rho} = \alpha t - \frac{\beta}{t} \qquad (2.21)$$

where the constants, $\alpha = \pi R^4 hg/8LV$ and $\beta = V/8\pi L$, depend only on the geometry of the viscometer tube. Measurement of the time required for the fixed volume V of two liquids of known viscosity and density to flow through the same tube is sufficient to define the viscometer constants, α and β. The viscosity of a liquid depends markedly on the temperature. Hence, the calibration measurements and the measurement of the viscosities of the polymer solutions must be made at the same carefully controlled temperature (± 0.1°C).

Since the ratios of viscosities will be relevant here, it is possible to divide both sides of equation (2.21) by α, giving a corrected efflux time equal to $t - (\beta/\alpha)/t$. Since β/α is typically the order of 100, the correction can be avoided entirely by choosing viscometer less than tolerable 1%.

The viscosities and densities of some typical solvents used in polymer chemistry are given in Table 2.4. It should be noted from (2.21) that the viscosities obtained from viscometer tube flow times are *kinematic* viscosities. The conversion of relative kinematic viscosity to relative viscosity can usually be made by assuming that the densities of solution and solvent are equal.

2.6.2.2.   Experimental apparatus

A number of methods exist for the determination of the viscosity of a liquid. The most useful method from the viewpoint of simplicity, accuracy, and cost is based on a measurement of the flow rate of the liquid through a capillary tube. In practice, the capillary tube forms part of the "viscometer."

The most commonly used viscometers are of the Ostwald and Ubbelohde types. In the Ostwald viscometer, shown in Figure 2.2, a given volume of liquid is introduced into B and is drawn up by suction into A until the liquid level is above the

Table 2.4 Densities and viscosities of common solvents (Allcock et al., 2003: 455).

Solvent	ρ (g/cm3) at:		100η (poises) at:	
	20°C	30°C	20°C	30°C
Benzene	0.8737	0.8684	0.652	0.564
Toluene	0.8669	0.8577	0.590	0.526
p-Xylene	0.8610	0.8523	0.644	0.568
Cyclohexane	0.7786	0.7693	0.935	0.820
n-Hexane	0.6594	0.6505	0.326	0.293
Ethanol	0.7893	0.7808	1.200	1.003
Acetone	0.7908	0.7793	0.326	0.295
Methyl ethyl ketone	0.8047	0.7945	0.400	0.365
Carbon tetrachloride	1.5940	1.5748	0.969	0.843
Chloroform	1.4892	1.4706	0.568	0.514

mark m_1. The suction is released and the time required for the liquid level to fall from m_1 to m_2 is measured. The average driving force during the flow of this volume of liquid through the capillary tube is proportional to the average difference in heights of the liquids in tubes B and A (i.e., proportional to h, as shown in Figure 2.2). In order that this driving force is the same in all cases, it is clearly essential that the same amount of liquid should always be introduced into tube B.
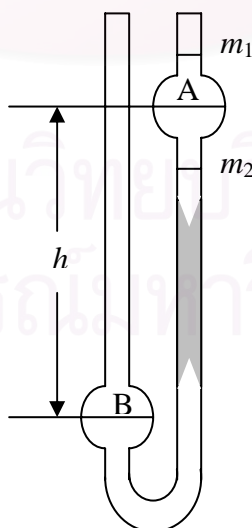
Figure 2.2 Ostwald viscometer.

2.6.3. Definition of solution-viscosity terms

The *relative viscosity*, which has already been defined in (2.14), may be written very simply in terms of the viscometer flow times if the kinetic energy correction is neglected:

$$\eta_r = \frac{\eta}{\eta_0} = \frac{t}{t_0} \tag{2.22}$$

where t and t_0 are for the flow of solution and solvent, respectively. Obviously, η and η_0 (i.e., t and t_0) must be measured under the same conditions. The relative viscosity is always greater than unity because the presence of the polymeric solute always increases the viscosity.

The best range experimentally is $\eta_r = 1.2\text{-}1.8$, because less than a 20% increase in viscosity is too difficult to measure reliably, and more than 80% could cause curvature in some of the extrapolations to infinite dilution that will be described.

It is appropriate, then, to define the *specific viscosity*, η_{sp}, as the fractional increase in viscosity caused by the presence of the dissolved polymer in the solvent, as shown in equation (2.23).

$$\eta_{sp} = \frac{\eta - \eta_0}{\eta_0} = \eta_r - 1 \tag{2.23}$$

The specific viscosity and the relative viscosity clearly depend on the concentration of the polymer in solution; they increase in magnitude with increasing concentration. The quantity η_{sp}/c, where c is the concentration of polymer in g/cm^3, is sometimes called the *reduced viscosity* or *reduced specific viscosity* and is a measure of the specific capacity of the polymer to increase the relative viscosity. Finally, the *intrinsic viscosity*, $[\eta]$, is defined as the limit of the reduced viscosity as the concentration approaches zero, and is given by

$$[\eta] = \lim_{c \to 0} \left(\frac{\eta_{sp}}{c} \right) \tag{2.24}$$

Note that none of the terms defined here actually has the dimensions of viscosity. The relative viscosity and the specific viscosity are dimensionless, but the reduced viscosity and the intrinsic viscosity have the dimensions of a specific volume (i.e., cm^3/g).

A linear dependence of the reduced viscosity on polymer concentration is usually found when $\eta_r < 2$. This linear dependence is described well by the expression

$$\frac{\eta_{sp}}{c} = [\eta] + k'[\eta]^2 c \qquad (2.25)$$

where k' is a constant, usually in the range 0.35 to 0.40; it is sometimes called the Huggins constant. In view of equation (2.24) and (2.25), it is evident that the intrinsic viscosity $[\eta]$ can be found by an extrapolation of the experimental values of the reduced viscosity (η_{sp}/c) to zero concentration. An alternative extrapolation replaces η_{sp}/c by η_r/c, and k' by k''.

2.6.4. Intrinsic viscosity and molecular weight

Suppose that the intrinsic viscosities $[\eta]_i$ (defined by equation 2.24) are determined for different molecular-weight fractions of a given polymer, each fraction having a very narrow range of molecular weights. Assume that the molecular weights, M_i, of the various fractions are known from the use of an absolute method such as ultracentrifugation or light scattering. It has been found that a straight line is obtained if the logarithms of the intrinsic viscosities are plotted versus the logarithms of the molecular weights of the different fractions. For a given polymer, the slope depends on the solvent. It is also found that, for a given polymer and solvent, the slope depends on the temperature.

Since a plot of $\log [\eta]_i$ versus $\log M_i$ is linear for narrow molecular-weight fractions of a given polymer, we may write

$$\log[\eta]_i = \log K + a \log M_i \qquad (2.26)$$

or

$$[\eta]_i = KM_i^a \qquad (2.27)$$

where K and a are constants that are easily determined from calibration plots. The relationship given in (2.27) is usually known as the Mark-Houwink equation.

It must be kept in mind that the data in the calibration plots, and equations (2.26) and (2.27), refer to fractionated samples of a given polymer, in which molecular-weight ranges of the fractions are very small. Carefully fractionated samples must be used in order to obtain numerical values for K and a for a given polymer-solvent pair at a given temperature. However, in practice, solution viscosity measurements are used to obtain, quickly and easily, a measure of the molecular

weight of an unfractionated or crudely fractionated polymer. An average molecular weight of the sample is obtained by this procedure and it is necessary to inquire about the type of average that is involved.

2.7.   Methane hydrate

Clathrate hydrates are well known structures that were considered for many years as harmful by the oil and gas industry because of their annoying tendency to plug pipelines (Chatti et al., 2005: 1333-1343). However, hydrates are now attracting renewed interest in many fields. Indeed, gas hydrates naturally found in deep seas and permafrost may provide a large amount of methane. Other positive applications include carbon dioxide sequestration, separation and natural gas storage and transportation. Finally, the use of their dissociation energy can be applied in refrigeration processes and cool storage.

Methane hydrate is a soft grayish ice, with a density of 0.91 gm/cm^3 (Chapman and Haynes, 2005: 372-383). It is unstable at STP (i.e., 0°C at 1 atm), but at higher pressures it is stable up to 17°C. Deposits are found only in the high Arctic, where subzero temperatures are maintained throughout the year. Arctic hydrate exists at depths of only a few hundred meters, so wells are shallow by oil-drilling standards.
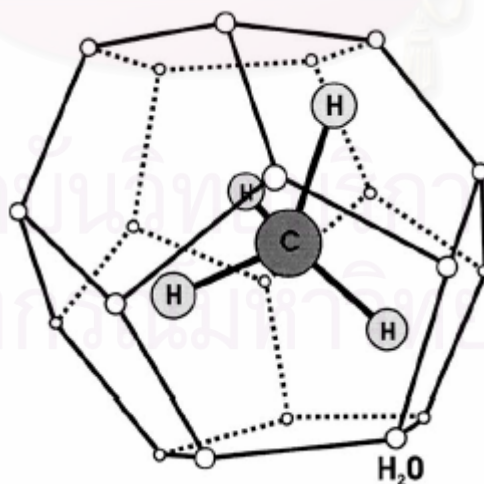

Figure 2.3   Methane hydrate: methane molecule (CH$_4$) imprisoned within the clathrate cage formed by water molecules (H$_2$O) (Beauchamp, 2004: 751-765).

Methane can be released in situ by lowering the pressure, applying heat, or pumping in antifreeze. Depressurization and thermal methods were successfully demonstrated in 2002 at the Mallik field on Richard's Island, in the Mackenzie River delta in Canada.

Hydrates are a surprisingly concentrated source of methane: $1m^3$ will release 170 m^3 of gas at STP. In other words, a chunk of hydrate contains as much methane as the same volume of gas at a pressure of 170 atm (2500 psi). For comparison, one cubic meter of liquid methane (boiling point $-161°C$) contains 622 m^3 of the gas at STP, less than four times more. The implication is that a hydrate deposit produces much more gas per unit volume accessed than a conventional natural gas well.

In some instances, it maybe desirable to mine the hydrate instead of releasing the gas. If a gas pipeline to market is not practical, the hydrate itself can be shipped if it is kept at 0°C and 150 psi. The hydrate is of course heavier than the gas it contains, by a factor of 8, but storing the gas in this form avoids the cryogenic refrigerator needed for liquid methane or the heavy tank needed for compressed gas.

Hydrates release a purer form of methane than that in natural gas at the wellhead, which typically contains 70–90% CH_4. The other constituents of natural gas are heavier alkanes (propane, ethane and butane) and small amounts of criteria pollutants such as hydrogen sulfide. The heavier alkanes are usually separated for sale in other markets, and most of the pollutants are removed during processing. As delivered to the consumer, "dry" natural gas is almost pure methane. Thus, gas from hydrates can substitute for natural gas without any modification of equipment.

Many energy companies are now actively involved in methane hydrate research. The US Methane Hydrate R&D Act of 2000 established a modest program (2004 authorization: US$12,000,000), coordinated by the Department of Energy. Japan, which lacks other domestic energy resources, is vigorously pursuing the technology needed to tap its extensive offshore hydrate deposits.

Knowledge about the extent of the worldwide deposits and the feasibility of extracting methane should improve greatly within the next 5 to 10 years. During that time, the only possible reason to proceed with development of the hydrogen economy is the concern that global warming is an urgent problem, demanding immediate action.

2.8.   Hypothesis

From the information that has been obtained, the author has then set up the hypothesis for this research as followed.

2.8.1.   In the photo-degradation process, the weight-average molecular weight of the natural rubber films should reduce with time.

2.8.2.   The following parameters should have significant effects on the reduction of the weight-average molecular weight of the natural rubber films.

- Light density

- Temperature

- Concentration of catalyst, peptizer, and retardant

2.8.3.   The kinetic model for the 1st order reaction with random chain scission can be applied to the photo-degradation of the natural rubber films.

2.8.4.   The number of double bonds in the natural rubber films should be able to be predicted by using the proposed method of calculation of double bonds in the natural rubber films.

Chapter III

Experimental Method

3.1.   Preparation of natural rubber films

The 60% DRC (dry rubber content) NR latex was used in the experiments. The catalysts, TiO_2 (anatase, Aldrich), and $K_2S_2O_8$ (Carlo Erba), were dispersed, or dissolved in distilled water, in which the concentration was varied from 0.1-1.5 phr (parts per hundred of rubber). The TiO_2 used was analyzed by using the Laser Analyzer to have a mean diameter of around 0.25 μm. The solution was agitated until it was well mixed. Then, the NR latex was poured into the solution, and the mixture was stirred by using a magnetic stirrer until totally mixed. Two grams of the mixture, having 50% DRC, were transferred to a flat-bottomed plastic container, having a dimension of 0.05 x 0.05 x 0.15 m (W x L x H), and then dried at 40°C in an oven for 24 hours. A 0.4 mm thick NR film was finally obtained.

3.2.   Apparatus

The experiments were carried out in a chamber, having a dimension of 0.50 x 0.52 x 0.60 m. A cooling bath made of zinc sheets, with an inside dimension of 0.28 x 0.38 x 0.15 m, and an outside dimension of 0.33 x 0.44 x 0.18 m, was placed in the chamber to control the temperature of the sample. A 400-watt mercury light bulb was installed at the front door of the chamber in a horizontal manner, 0.05 m above the top of the cooling bath. The temperature of the sample was measured by placing a thermocouple on the surface of the sample.

3.3.   Photo-degradation of natural rubber films

The NR films with and without catalysts were exposed to light, which had the density of 7,000 and 36,000 lux, at the temperatures of 25°C and 80°C for 192 hrs. The samples were collected at various intervals, and were kept in a dry cool dark place.

3.4.   Molecular weight analysis

The NR films, before and after exposure, were dissolved in the tetrahydrofuran (THF, HPLC grade), and filtered through 0.45-μm PTFE filters. The

rubber solution with a concentration of 1 g/l was injected into the GPC system (Waters Corp.), which was composed of an isocratic HPLC pump that pumped THF at a flow rate of 1 ml/min, three Styragel columns with different sizes, and an online refractive index detector. The chromatograph of the sample injected into the GPC provided the signal intensity versus retention time, which was then converted into *Mw*.

3.5. Functional groups analysis

The NR films were dissolved in the toluene for 24 hrs. The solution obtained was cast on a sodium chloride cell and dried to get a thin film. Then the sodium chloride cell with the thin film was inserted into the FTIR (Thermo) to analyze the functional groups of the NR.

3.6. Tensile strength analysis

The analysis of tensile strength of the NR films was done accordingly to the ASTM D412-06.

3.7. Analysis of viscosity of rubber solution

The NR films were dissolved in toluene at several concentrations, and the solution viscosity was measured following ASTM D445-06, at the temperature of 35°C.

3.8. Surface characteristic study of the natural rubber films

The surface characteristics of the NR films were studied using the microscope (Olympus).

3.9. Analysis of moisture content in the natural rubber films

The NR films were dried in an oven at 50°C until their weights did not change. The difference of the weight of the NR films before and after drying is the weight of moisture contained in the NR films.

3.10. Analysis of gas permeability of the natural rubber films

The pure NR films were tested for the gas permeability using the Capillary

Flow Porometer (Porous Material, Inc.), model CFP-1100-A. The gas used for this test is nitrogen gas.

3.11.   <u>Simulation of the utilization of the natural rubber films at low temperature</u>

The NR films were used to store the ice at the temperature below 0°C, and kept at this condition for at least 30 days. The tested NR films were observed for changes.

Chapter IV

Results and Discussion

4.1. Photo-degradation of natural rubber films

4.1.1. Initial study: 2^k experimental design

First of all, the interesting factors, which are catalyst concentration, light density, and time, were studied if they have any significant effects on the photo-degradation process of the NR films. Therefore, the 2^k experimental design with three variables, which are stated above, was carried out. The catalyst used in this experiment was TiO_2. The condition applied is shown in Table 4.1.

Table 4.1 The condition used in the first experiment.

		Factor level	
	Effect	Low (-1)	High (+1)
TiO_2 (phr)	A	0	2
Light density (lux)	B	0	36,000
Time (hrs)	C	24	48
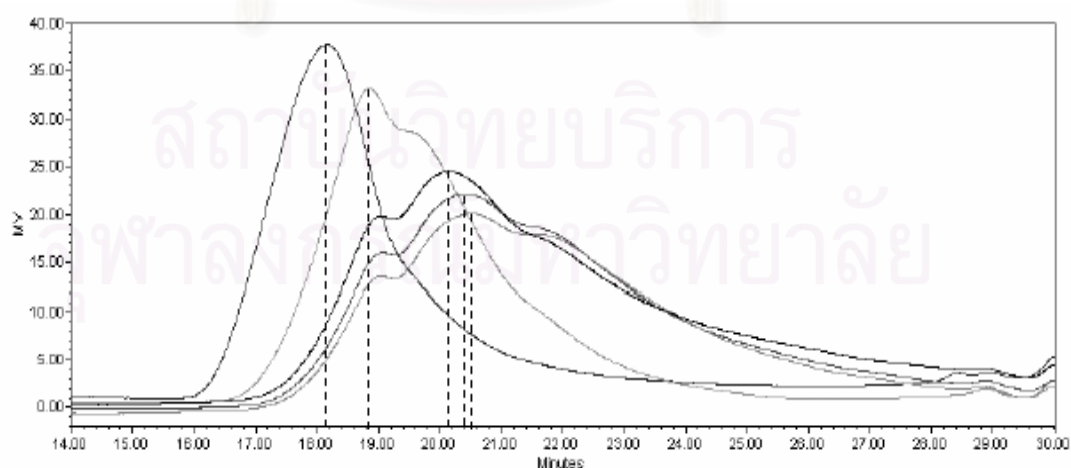
Figure 4.1 GPC chromatograms of NR + TiO_2 0.1 phr exposed to light for 0, 48, 96, 144, and 192 hrs from left to right, respectively.
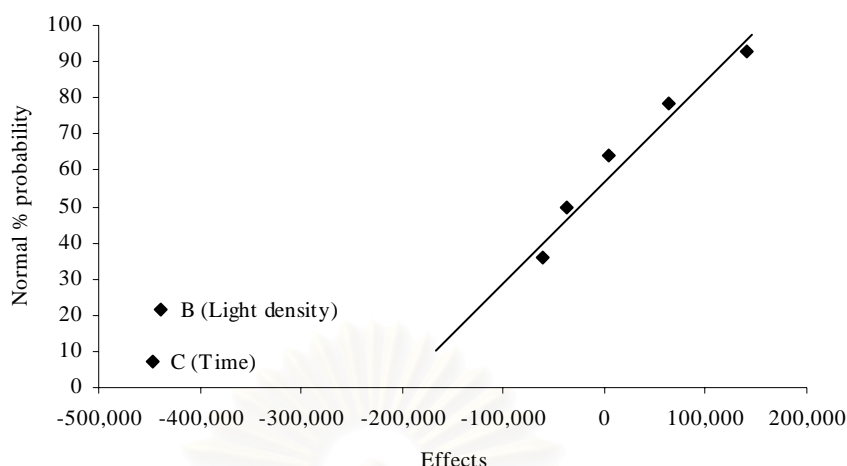
Figure 4.2   Normal probability plot of the effects in the first experiment.

The 0.4 mm thick NR films prepared from the NR latex were placed in the chamber with a 400-watt mercury light bulb installed, but without the cooling bath. After exposed to light for a period of time being set, the NR films were taken out to analyze the *Mw* by using the GPC. Then the set of *Mw* obtained was calculated using the 2^k experimental design method to see if the interesting factors have any effects on the photo-degradation of the NR films.

Figure 4.1 shows the GPC chromatograms obtained by injecting the NR samples, which were exposed to light for different periods of time. More retention time represents less *Mw*. The *Mw* obtained was then used in the 2^k experimental design calculation. The normal probability plot in Figure 4.2 shows that light density and time have significant effects on the photo-degradation of the NR films in the first experiment. But the plot of residuals versus *Mw* shown in Figure 4.3 seems to have a pattern, which means there might be something unusual.

So the test results shown in Figure 4.4 was reconsidered, and found that at the light density of 0 lux (or no light), the *Mw* of the NR films decreased with time, which was unexpected. This was because the light bulb generated a lot of heat, and the heat could not be transferred out easily from the closed chamber. Therefore, the temperature in the chamber rose up to 60°C, which was high enough to degrade the rubber.
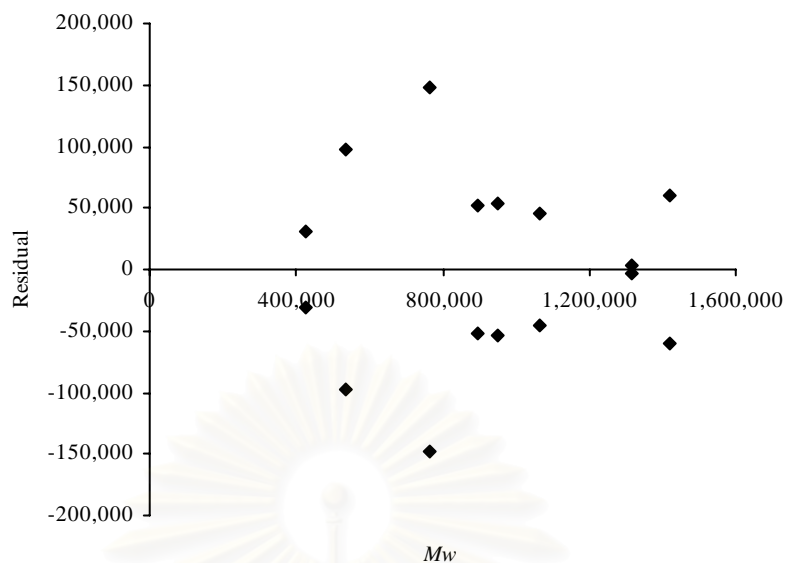
Figure 4.3   Plot of residuals versus average molecular weight in the first experiment.

Figure 4.4   Effects of light density (0-36,000 lux), exposure time (24-48 hrs), and concentration of TiO_2 (0-2 phr) on the reduction of Mw in the first experiment. (The error bars represent the minimum and maximum values of Mw data.)

Since the temperature in the chamber could affect the test results, the cooling bath was introduced to the second experiment to control the temperature of the samples to around 25°C. The condition used in the second experiment is shown in Table 4.2.

Table 4.2 The condition used in the second experiment.

		Factor level	
	Effect	Low (-1)	High (+1)
Light density (lux)	A	0	36,000
Time (hrs)	B	24	48
TiO_2 (phr)	C	0	0.5

The normal probability plot of the effects in the second experiment, shown in Figure 4.5, exhibits that light density, time, and the interaction between light density and time have significant effects on the photo-degradation process.
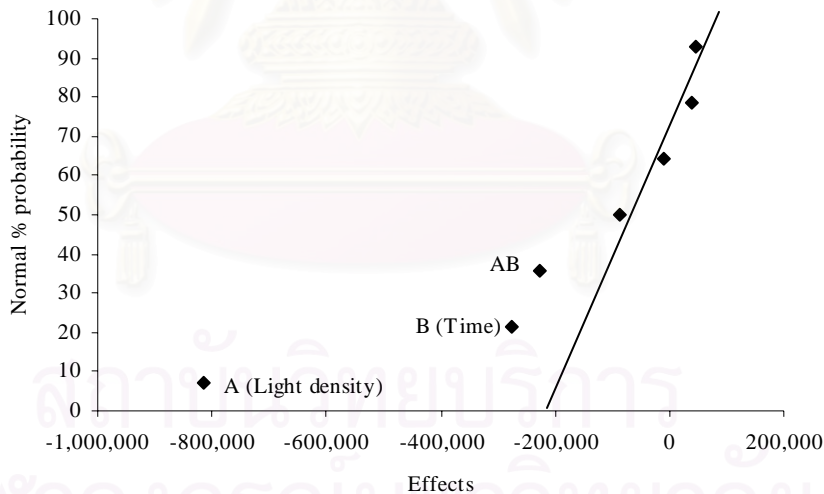
Figure 4.5   Normal probability plot of the effects in the second experiment.

Figure 4.6 demonstrates the interaction between light density (A) and time (B) in the second experiment. When the light density is low, the Mw does not change much whether when the exposure time is short or long. But when the light density is high, the exposure time has a significant effect in that the longer time can help decrease more Mw of the NR films than the shorter time does.

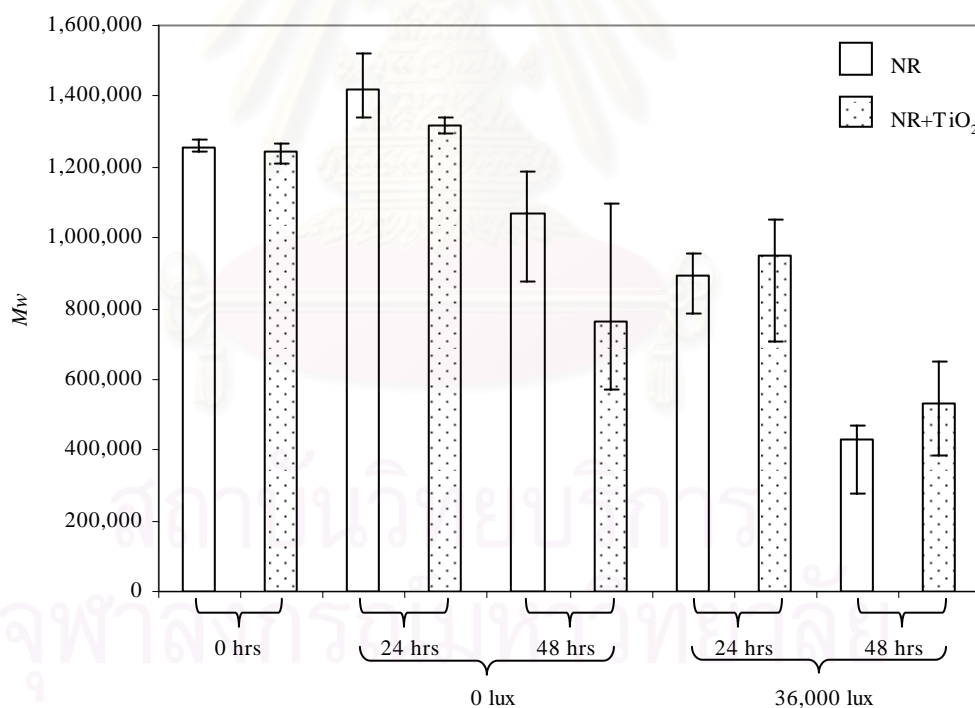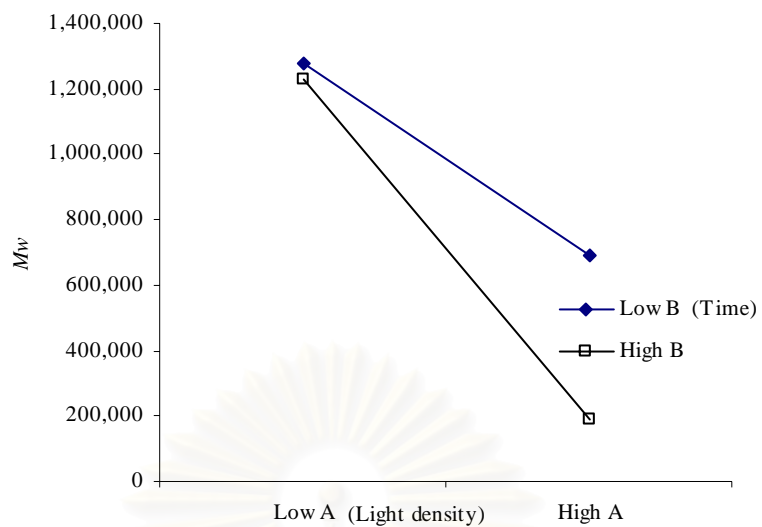Figure 4.6   Plot of AB interaction in the second experiment.
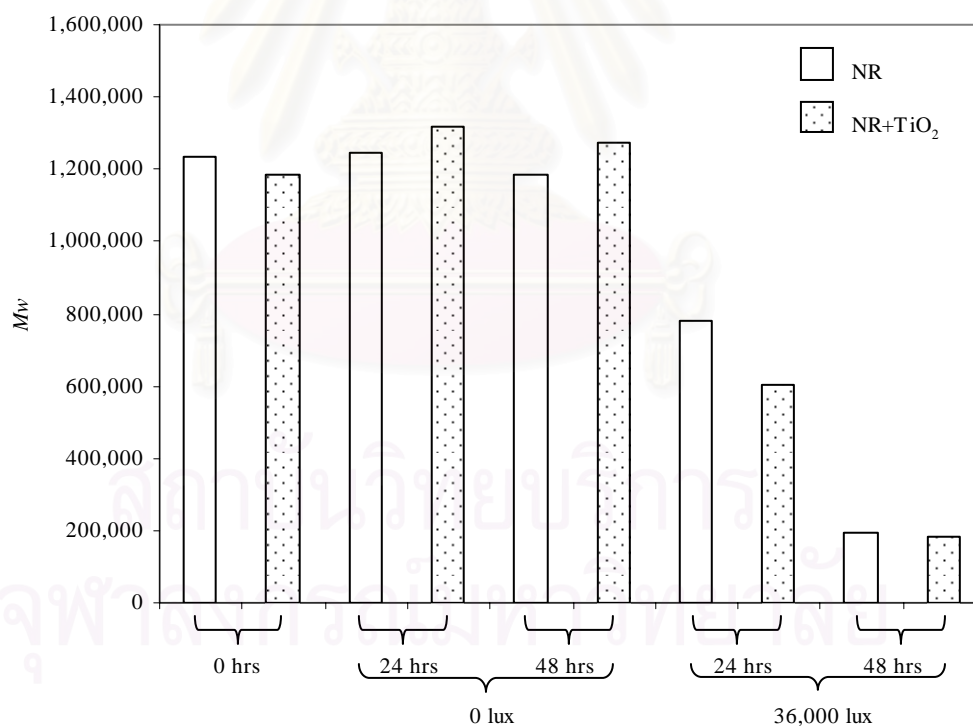
Figure 4.7   Effects of light density (0-36,000 lux), exposure time (24-48 hrs), and concentration of TiO_2 (0-0.5 phr) on the reduction of Mw in the second experiment.

After improving the temperature control system by using the cooling bath, more sensible results were obtained. It can be seen from Figure 4.7 that at the light density of 0 lux, the *Mw* of the NR films does not have much different even when the exposure time gets longer. On the other hand, at the light density of 36,000 lux, it is obvious that the *Mw* of the NR films reduces quite quickly at longer exposure time.

Even though the experimental results showed that the concentration of TiO_2 does not have significant effects on the photo-degradation of the NR films, the author was still interested in doing some tests on the type and concentration of catalysts. So the next experiment was done by varying the type and concentration of catalysts to see if different types and concentrations of catalysts in the interesting range have any effects on this degradation process.

4.1.2. Variation of type and concentration of catalyst

First of all, a wide range of catalyst concentration was tested. The condition used in this experiment is as shown below.

Type of catalyst	:	TiO_2, $K_2S_2O_8$
Catalyst concentration (phr)		
TiO_2	:	1, 2, 4, 8
$K_2S_2O_8$	:	0.05, 0.5, 1, 2
Light density (lux)	:	36,000
Temperature (°C)	:	25
Exposure time (hrs)	:	0, 24, 48, 96, 192

After the NR films were exposed to light up to 192 hrs, They were tested for the *Mw*. Since the solutions of the rubber exposed to light from 0 to 96 hrs, which were prepared for GPC test, were left for approximately two weeks, the dissolved rubber molecules might have been degraded. Therefore, some *Mw* values are too low. But for the fresh rubber solutions prepared from the 192-hr exposed NR films, a tendency of *Mw* result was obtained, as shown in Figure 4.8.
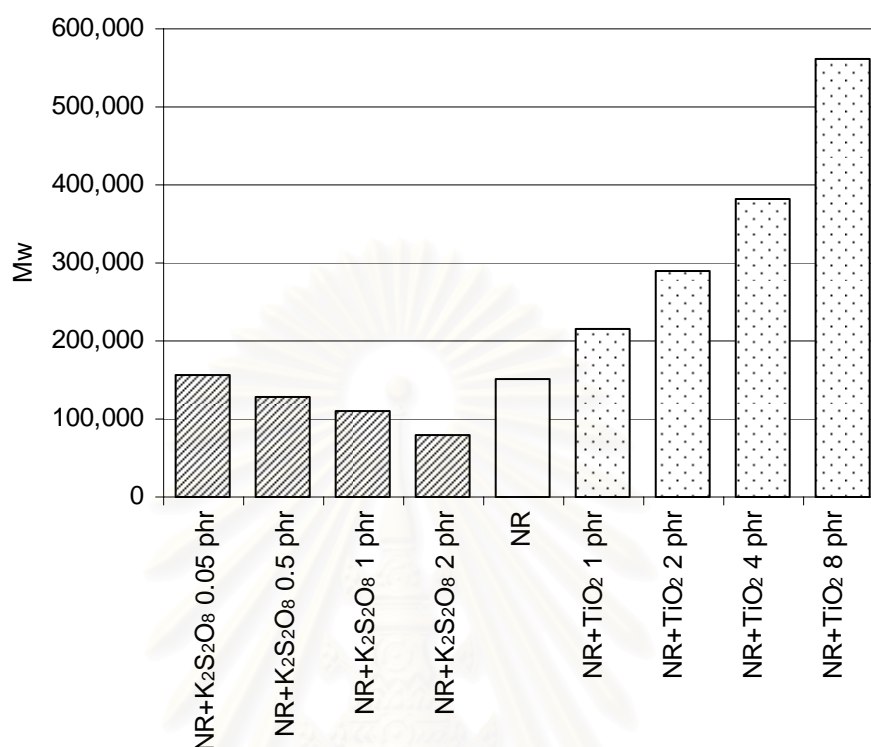
Figure 4.8   Weight-average molecular weight of natural rubber films with and
without catalysts, at 192 hrs of exposure time, 36,000 lux, 25°C.

For the NR films with $K_2S_2O_8$, the *Mw* tends to decrease a little bit when the
concentration of $K_2S_2O_8$ is higher, which means that $K_2S_2O_8$ might be able to act as a
catalyst in this photo-degradation process. But its concentration cannot be increase to
more than 2 phr, because it tends to saturate and crystallize on the films.

Considering the results of NR with TiO_2, it is very obvious that more TiO_2 can
reduce the *Mw* reduction of the NR films. This is probably because the TiO_2 can also
act as a stabilizer (Turton and White, 2001), as it can block the penetration of the
light. So the more concentration of TiO_2 can lead to the slower rate of photo-
degradation of the NR.

4.1.3. <u>Effect of type and concentration of catalyst on photo-degradation of</u> <u>natural rubber films</u>

This experiment was carried out at almost the same condition as above, only the concentration of catalysts was change. The concentration of TiO_2 was reduced to see if less concentration can affect the photo-degradation of the NR films. And the concentration of $K_2S_2O_8$ was divided into a narrow range to see if there is any effect on the degradation. The experimental condition is as shown below.

Type of catalyst   : TiO_2, $K_2S_2O_8$
Catalyst concentration (phr)
        TiO_2 :   0.1, 0.2, 0.5, 0.7, 1.0
        $K_2S_2O_8$:   0.1, 0.2, 0.5, 0.7, 1.0, 1.5
Light density (lux)   :   36,000
Temperature (°C)   :   25
Exposure time (hrs)   :   0, 24, 48, 96, 192

From the relationship between the *Mw* and the exposure time in Figure 4.9, the *Mw* of all NR samples decreases with time, and seems to be constant after 96 hrs. For the NR samples with TiO_2, all the curves have almost the same tendency, except those with TiO_2 0.5-1 phr, which tend to have a little bit slower degradation rates than others. As mentioned above, this is probably because the TiO_2 can also act as a stabilizer (Turton and White, 2001), as it can block the penetration of the light. So the more concentration of TiO_2 can lead to the slower rate of photo-degradation of the NR. On the other hand, more concentration of $K_2S_2O_8$ tends to reduce more *Mw* from the time that the films were not exposed. This may not be acceptable in the aspect of the stability for the reason that the NR films should not degrade before used. Therefore, the catalyst concentration chosen for further experiment is 0.1 phr.
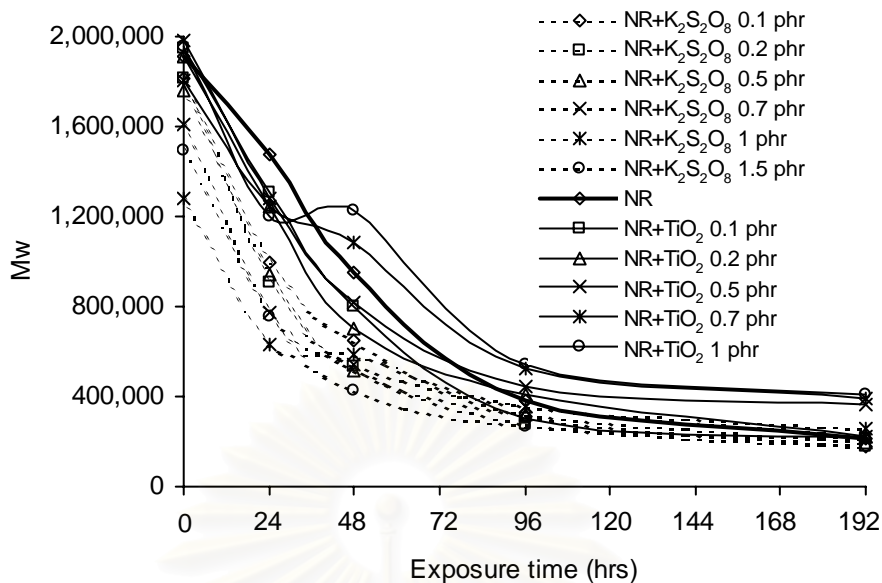
Figure 4.9   Weight-average molecular weight reduction of natural rubber films with
and without catalysts, at 36,000 lux, 25°C.

4.1.4. Effect of temperature on photo-degradation of natural rubber films
The experiment was carried out following the condition below.

Type of catalyst   : TiO_2, $K_2S_2O_8$
Catalyst concentration (phr)
  TiO_2 :   0.1
  $K_2S_2O_8$:   0.1
Light density (lux)   :   36,000
Temperature (°C)   :   25, 80
Exposure time (hrs)   :   0, 24, 48, 72, 96, 144, 192

From the photo-degradation of NR films at the light density of 36,000 lux, and
at the temperature of 25°C and 80°C, as shown in Figure 4.10, it can be observed that
the NR samples tested at 80°C have a faster degradation rate than the ones tested at
25°C. This is probably because the higher temperature provides more heat energy to
excite the molecules, and that it gives more opportunities for many degradation
reactions to occur in a faster rate. This is consistent with a study on degradation of

polyethylene films (Andrady et al., 1998: 96-103). The *Mw* reduction seems to stop at the exposure time of 144 hrs at 25°C, and 96 hrs at 80°C, respectively.
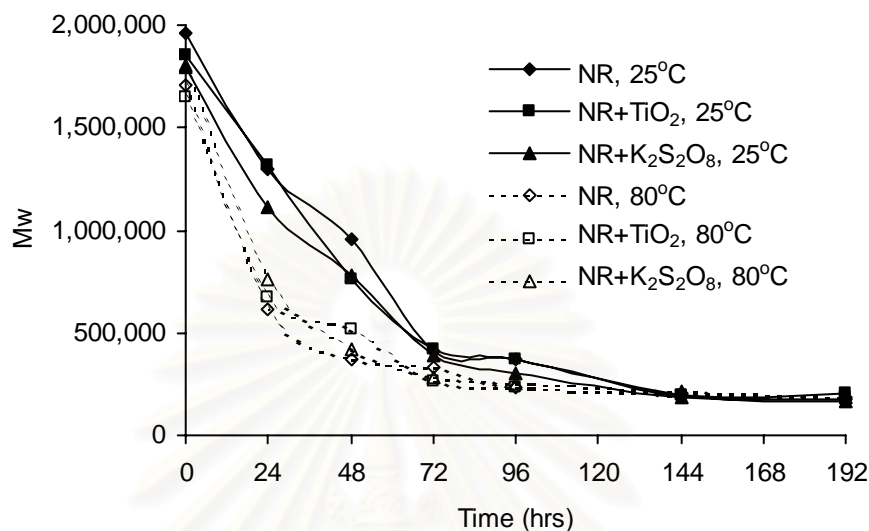
Figure 4.10   Average molecular weight reduction of natural rubber films with and without catalysts 0.1 phr, at 36,000 lux, 25°C and 80°C.

Comparing the results tested at the same catalyst concentration of 0.1 phr in Figure 4.10, it can be observed that the NR samples with and without catalysts, TiO_2 and $K_2S_2O_8$, give quite similar results. Actually, the samples with catalysts, especially TiO_2, are expected to have a faster degradation rate than that without catalysts as shown in some other works, such as Cho (2001) and Shang's (2003a, 2003b) works, which used TiO_2 as a photo-catalyst in the photo-degradation process of some polymers. There may be several factors that make the results of each sample become the same, such as the thickness of the films, the experimental condition, and the types of polymers. Shang et al. (2003b) pursued the photo-degradation of polystyrene (PS) plastic with TiO_2 as a photo-catalyst. The PS plastic was made into thin films having a thickness of 35 μm. The result showed that the PS-TiO_2 sample degraded more quickly than the PS sample. It was claimed that the degradation initially occurred over TiO_2 particles, followed by the diffusion reaction with the aid of reactive oxygen species generated on TiO_2 particle surfaces. Compared to Shang's work, the NR films (0.4 mm thick) used in the authors' work were much thicker than those of Shang's. The light and oxygen molecules might not be able to penetrate very deeply through

the films. So, the degradation reaction occurred mainly on the surface of the films. In the *Mw* analysis, the NR films were cut into pieces, from the surface through the bottom, and the whole piece was dissolved in THF prior to the analysis. Therefore, the *Mw* obtained was the *Mw* of the whole piece of the NR sample. This probably makes the overall results become quite similar.

4.1.5. Effect of light density on photo-degradation of natural rubber films

The photo-physical processes involved in photo-degradation include absorption of light by material, electronic excitation of the molecules, and deactivation by radiation or radiationless energy transitions, or by energy transfer to some acceptor. (Kelen, 1983: 137-138) When the lifetime of the excited state is sufficiently long, the species can participate in various chemical transformations. The absorption of light results in an electronic transition between two energy levels in the absorbing molecule; this absorbed energy is exactly equal to the energy of a light quantum:

$$E = nh\nu \qquad\qquad (4.1)$$

where h is Planck's constant, ν is the frequency of the absorbed light, and n is the number of photons. More light density means more quantity of light, or more number of photons, which leads to more energy. This is consistent with the results of the experiments in this section, which were carried out at $25^{\circ}C$ by placing two pieces of black cloths in between the light bulb and the samples to reduce the light density to 7,000 lux. According to Figure 4.11, the result shows that the rate of *Mw* reduction of the NR films exposed to light at 36,000 lux is much faster than that at 7,000 lux. Because more light density gives more energy to make the NR become more excited, more degradation reactions can occur.
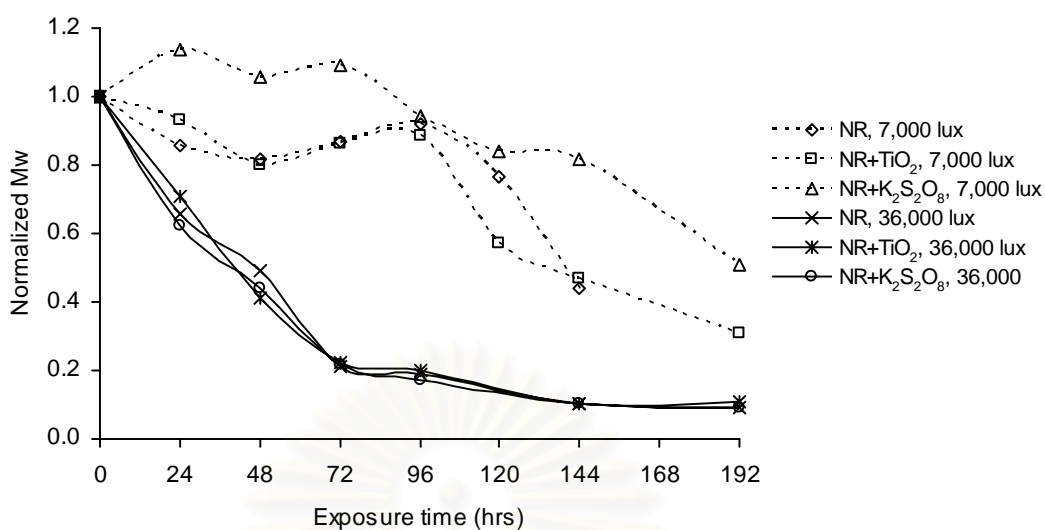
Figure 4.11   Normalized *Mw* of natural rubber films with and without catalysts 0.1 phr, at 7,000 and 36,000 lux, 25°C.

4.1.6. Double bonds reduction in natural rubber films

The number of double bonds in the NR films was calculated, on the basis of 1 kg of NR, by using the calculation method as mentioned in Chapter II.

The results from the calculation using the equations above are plotted in Figure 4.12 and 4.13. Figure 4.12 shows the reduction of calculated double bonds in NR films with and without catalysts 0.1 phr, at the light density of 36,000 lux, and at the temperatures of 25°C and 80°C. The trends of all curves are quite the same, and are similar to the curves of Adam (1991) and Santos's (2005) works (Figure 4.14, 4.15). The catalysts seem not to have much effect on the reduction of double bonds, but the high temperature has a significant effect in that it provides a faster rate of reduction of double bonds than the lower one does. This is consistent with the *Mw* reduction at the same condition, which is reported above. When the light density is decreased to 7,000 lux, at the temperature of 25°C, the rate of reduction of double bonds is much slower than that at 36,000 lux, as shown in Figure 4.13. This may be explained that less light density gives less energy to excite the molecules. Thus, the NR samples can resist the degradation longer than those tested at higher light density.
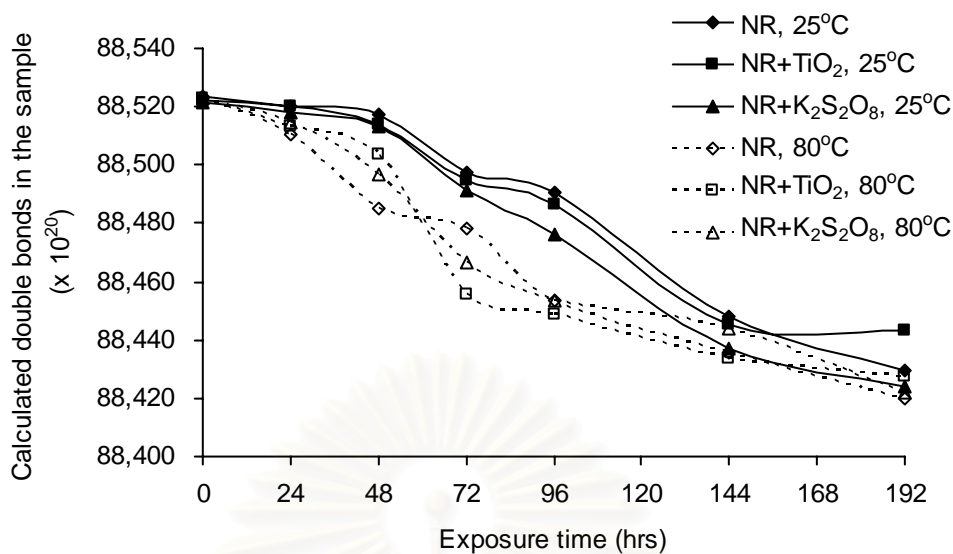
Figure 4.12   Reduction of calculated double bonds in natural rubber films with and without catalysts 0.1 phr, at 36,000 lux, 25°C and 80°C.
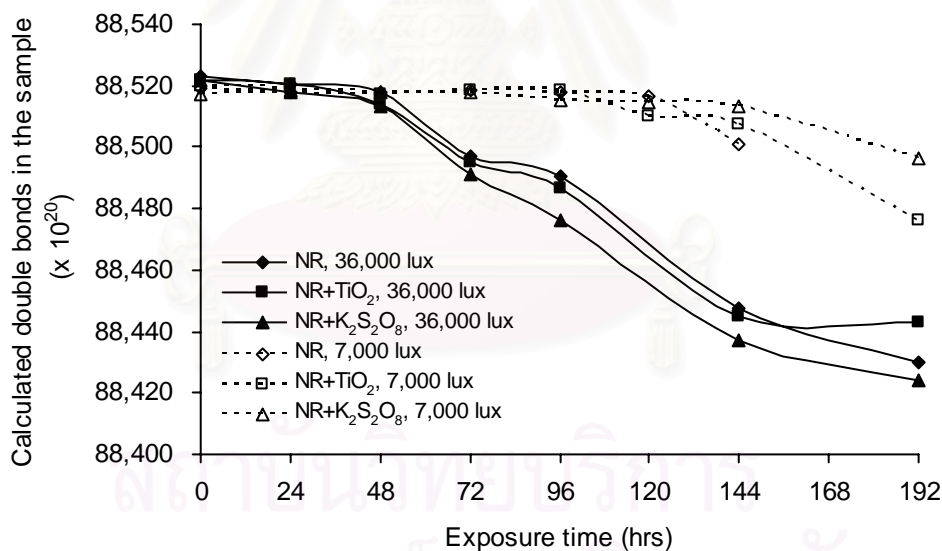
Figure 4.13   Reduction of calculated double bonds in natural rubber films with and without catalysts 0.1 phr, at 7,000 and 36,000 lux, 25°C.

Comparing the amount of the double bonds in this work with Adam and Santos's works, the percentages of the double bonds reduction are markedly different. This is probably due to the difference between the thicknesses of the films in each

work, as mentioned before. The NR films in this work are much thicker than those in the others' works that they might be degraded only on the films surface. Nevertheless, the comparable patterns of all curves exhibit that the calculation of the amount of double bonds in this work may possibly be used.
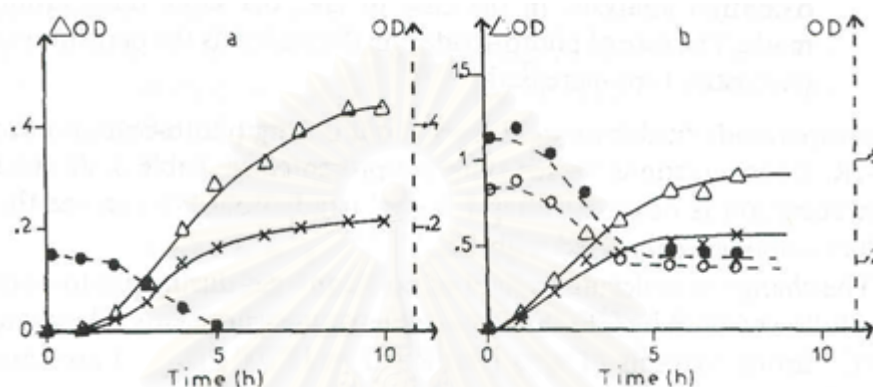
Figure 4.14   Formation of photo-products and consumption of double bonds versus time. (a) Polyisoprene with 98% 1-4 *cis*; (b) polyisoprene with 69% 1-4 *cis*, 23% 1-4 *trans*, 14% 3-4 structure. ($\triangle$) Carbonyl photo-products; ($\times$) hydroxyl photo-products; ($\bullet$) 1,4 double bond; ($\square$) 1,2 double bond; ($\bigcirc$) 3,4 double bond (Adam et al., 1991: 61).
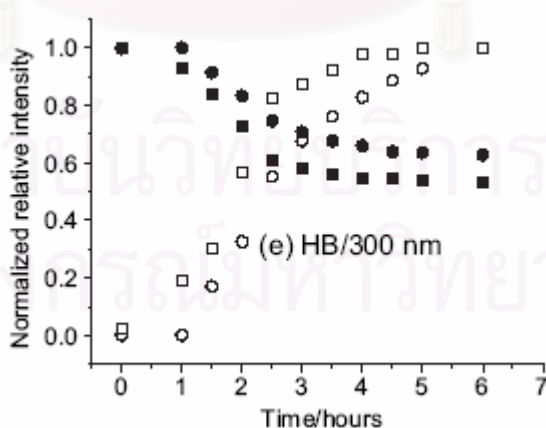
Figure 4.15   Dependence of FTIR intensities of ($\bigcirc$) C=O stretching, ($\bullet$) C=C stretching, ($\square$) O–H stretching, and ($\blacksquare$) =C–H wag vibrational modes of natural rubber at 300 nm UV irradiation (Santos et al., 2005: 38).

4.1.7.   Kinetic aspect of the photo-degradation of natural rubber films

The photo-degradation of NR films was followed experimentally by determination of the *Mw* as a function of time, using GPC technique. This technique can be applied only as long as the *Mw* remains large; i.e., in terms of the number of bonds broken, which involves a study of the initial stages of the reaction only (Tanford, 1961). A first-order rate equation (2.7), which has been explained in Chapter II, for random scission of a macromolecule was used here. If the plot of 1/*Mw* versus time of the initial stage of the degradation is linear, it demonstrates the first-order reaction. This equation has been used in some literature such as the enzymatic degradation of oat β-glucan (Roubroeks et al., 2001: 275-285).

The plots of 1/*Mw* versus the exposure time of the NR films with TiO_2 0.1 phr at the light density of 36,000 lux, and at the temperatures of 25°C and 80°C are shown in Figure 4.16. The linear plots of the initial stages of the degradation exhibit the pseudo first-order reactions. Even though it is claimed in Santos's (2005) work that cross linking and polymer reticulation can also occur in the photo-degradation process, but from the linear plots, it is quite obvious that photo-degradation of NR films in the present work is the pseudo first-order reaction, which the random chain scission reaction occurs preferentially. The calculated rate constants are shown in Table 4.3. The rate of the reaction at 80°C is faster than that at 25°C. The same tendency is obtained for the pure NR films and the ones with $K_2S_2O_8$ 0.1 phr, which
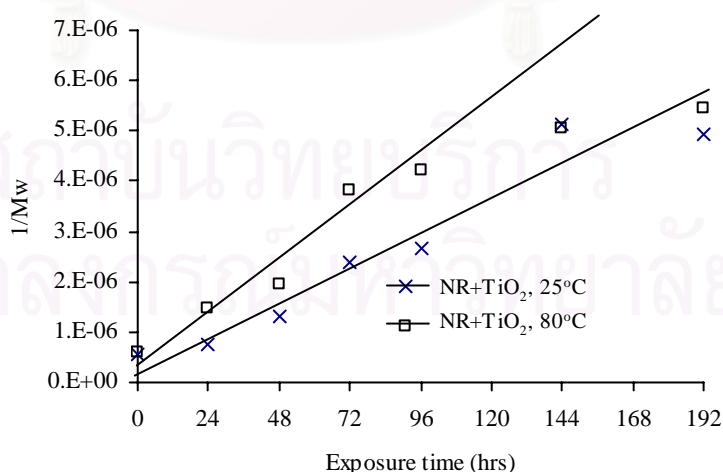
Figure 4.16   Reciprocal of *Mw* of NR films with TiO_2 0.1 phr plotted as a function of degradation time (at 36,000 lux).

demonstrates that these degradation processes are pseudo first-order reactions with random chain scission.

Table 4.3   Rate constants calculated at the initial stages of degradation (0-96 hrs) of NR films with and without catalysts 0.1 phr, at 36,000 lux.

	k (hr^{-1})	
	25°C	80°C
NR	2.72E-06	5.44E-06
NR+TiO$_2$	2.72E-06	5.44E-06
NR+K$_2$S$_2$O$_8$	4.08E-06	5.44E-06

4.2.   Tensile strength analysis

Tensile strength is one of the important properties of NR. The objectives of the test in this section are

1)   to prove that the natural rubber films that are exposed to light are degraded, which is consistent with the *Mw* reduction

2)   to prove that the addition of vulcanizing agent can help reinforce the natural rubber films

3)   to study the rubber vulcanization simultaneously with the photo-degradation.

The NR films used in this experiment were divided into 4 types:

A   NR

B   NR + K$_2$S$_2$O$_8$ 0.1 phr

C   NR + vulcanizing agent

D   NR + vulcanizing agent + K$_2$S$_2$O$_8$ 0.1 phr

The composition that was used as the vulcanizing agent in this experiment is as shown below.

10% KOH (potassium hydroxide)

Sulfur* in TMTD (Tetramethyl thiuram disulfide)

ZDEC (Zinc diethyl dithiocarbamate)

ZnO (Zinc oxide)

* The TMTD can provide 13% sulfur

The experimental condition in this section is as followed

Catalyst

$K_2S_2O_8$ 0.1   phr

Vulcanizing agent

10% KOH   1   phr

S in TMTD   2   phr

ZDEC   3   phr

ZnO   3.5   phr

Light density (lux)   :   36,000

Temperature (°C)   :   80

Exposure time (hrs)   :   0, 72

The vulcanizing agent and catalyst were mixed with the NR latex, and stirred until it was well mixed. After that, the rubber solution was poured on a glass plate, and dried at 50°C to make a film. Then the rubber films were exposed to light, and collected to make a tensile strength test.

All types of NR, A, B, C, and D, as mentioned above, were made into films before exposed to light. In addition, in order to study the rubber vulcanization simultaneously with the photo-degradation, the NR type C and D were not made into films before exposure, which means they were exposed to light from the time they were solutions to see what would happen if the photo-degradation occurs simultaneously with the vulcanization.

The analysis results of tensile strength were displayed in Figure 4.17. For the unexposed NR films, the films type A and B have quite similar tensile strength, as well as type C and D. On the other hand, type A and B have much lower tensile strength than type C and D. This is because type C and D have the vulcanizing agent in the composition, which it can help reinforce the NR films. After exposure for 72 hrs, the films type A and B were degraded until the films became sticky and could not be tested for the tensile strength. Only the films type C and D could be tested. From the results, the film type D has lower tensile strength than type C. This is probably because $K_2S_2O_8$ can help break down the rubber molecule. For the films type C and D that were not dried before exposure (C and D simultaneous), the tensile strength

values are quite similar to those of type C and D that were dried before exposure. This exhibits that the photo-degradation simultaneously with the vulcanization does not have significant effect on the tensile strength or on the degradation process. But at the same time, it shows that the rubber can still be vulcanized even it is photo-degraded.
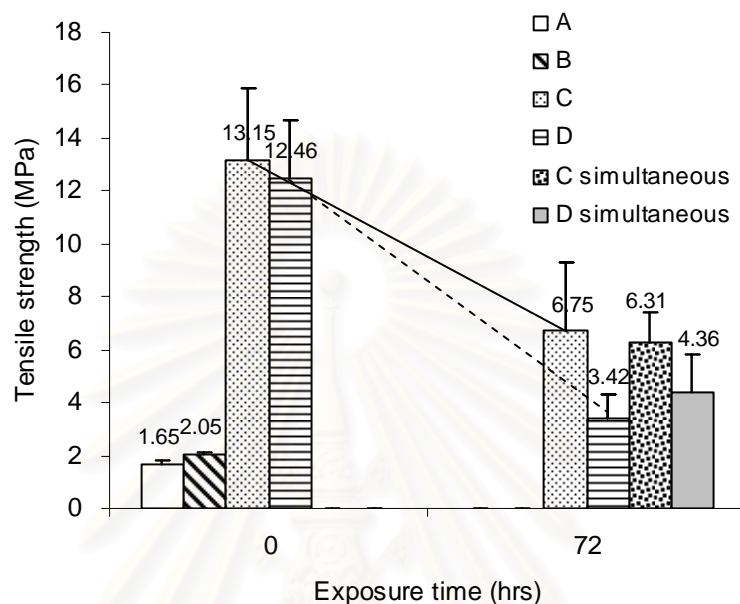
Figure 4.17   Tensile strength of the NR films plotted as a function of degradation time, at 80°C, 36,000 lux. (The error bars represent the standard deviation values.)

Considering the elongation at break of the NR films (Figure 4.18), before exposure, we can see that the films type A, B, C, and D do not have much different values. After exposure, the elongations at break are reduced. The values of type C and D are quite similar to those of C and D simultaneous.

From tensile strength test results it is obvious that the NR films can be photo-degraded which is consistent to the *Mw* reduction results. The vulcanized NR films were then characterized by using the microscope (Olympus). At the magnification of 10X, we can see the cracks on the surface of the NR film (Figure 4.19). The cracks are even more visible when the film is a little bit stretched (Figure 4.20). From another point of view, these cracks that appear on the NR films surface might be beneficial in that the weaken films surface can probably react with other chemicals easily, and all these cracks can help increase the reacted surface area of the films.
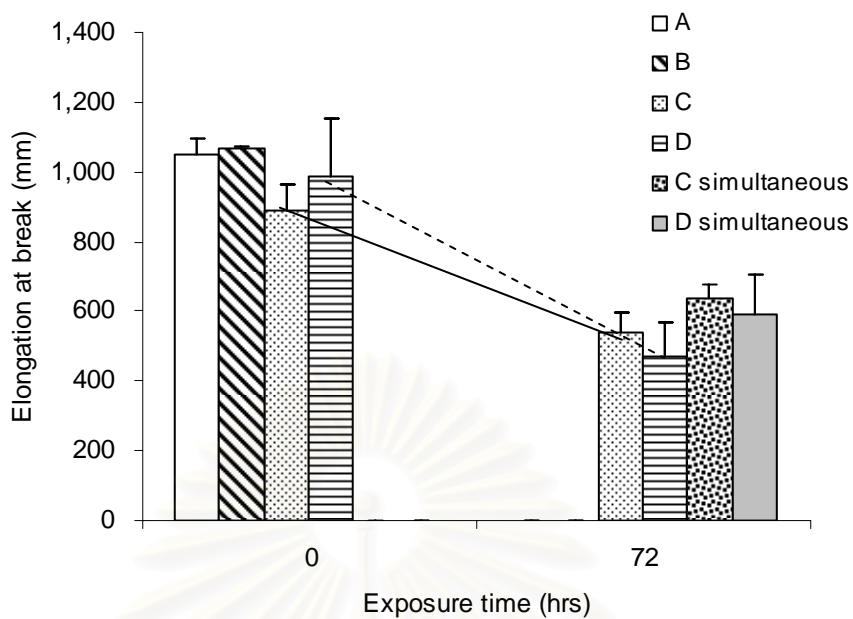
Figure 4.18   Elongation at break of the NR films plotted as a function of degradation time, at 80°C, 36,000 lux. (The error bars represent the standard deviation values.)

Figure 4.19   Cracks on the surface of vulcanized NR film at the magnification of 10X.

Figure 4.20   Cracks on the surface of stretched vulcanized NR film at the magnification of 10X.

4.3.   Surface characteristic of natural rubber films

The NR films, before and after exposure, were characterized by using the microscope to see the appearance of the films surface. The NR films used in this section were the films photo-degraded at the following condition.

Type of catalyst	:	TiO_2, $K_2S_2O_8$
Catalyst concentration (phr)		
TiO_2	:	0.1
$K_2S_2O_8$	:	0.1
Light density (lux)	:	7,000
Temperature (°C)	:	25
Exposure time (hrs)	:	0, 24, 48, 72, 96, 144

The characterization results of the pure NR films, NR +TiO_2 0.1 phr films, and NR + $K_2S_2O_8$ 0.1 phr films are shown in Figure 4.21, 4.23, and 4.24, respectively. Numerous small shallow holes are markedly seen on the films surface. Before exposure, the holes are still very small. These small holes might be formed by water evaporation in the process of film casting. After exposure, the degradation occurs,
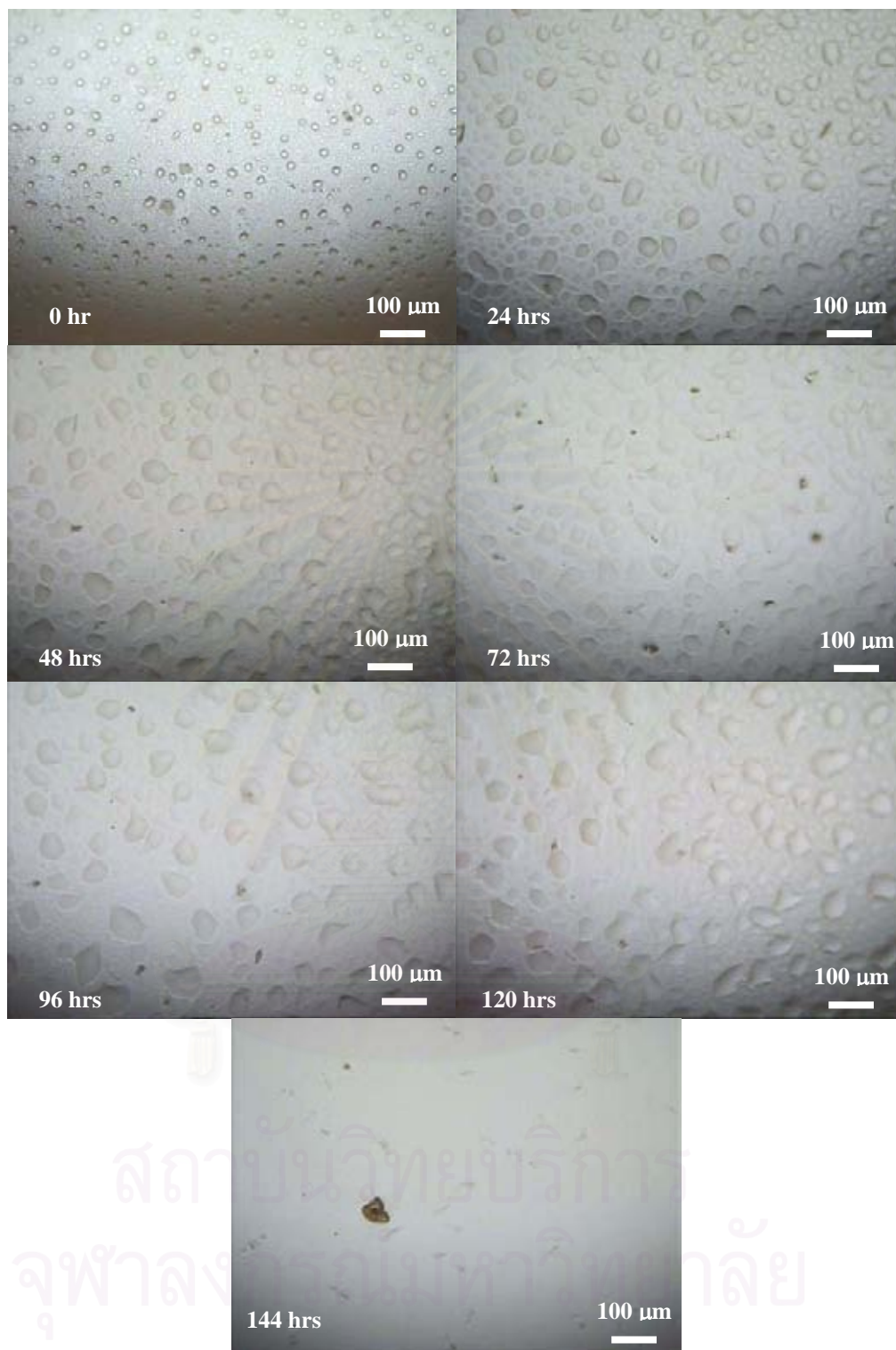
Figure 4.21   Surface characteristic of the pure NR films photo-degraded at different
exposure time at the magnification of 20X. (25°C, 7,000 lux)
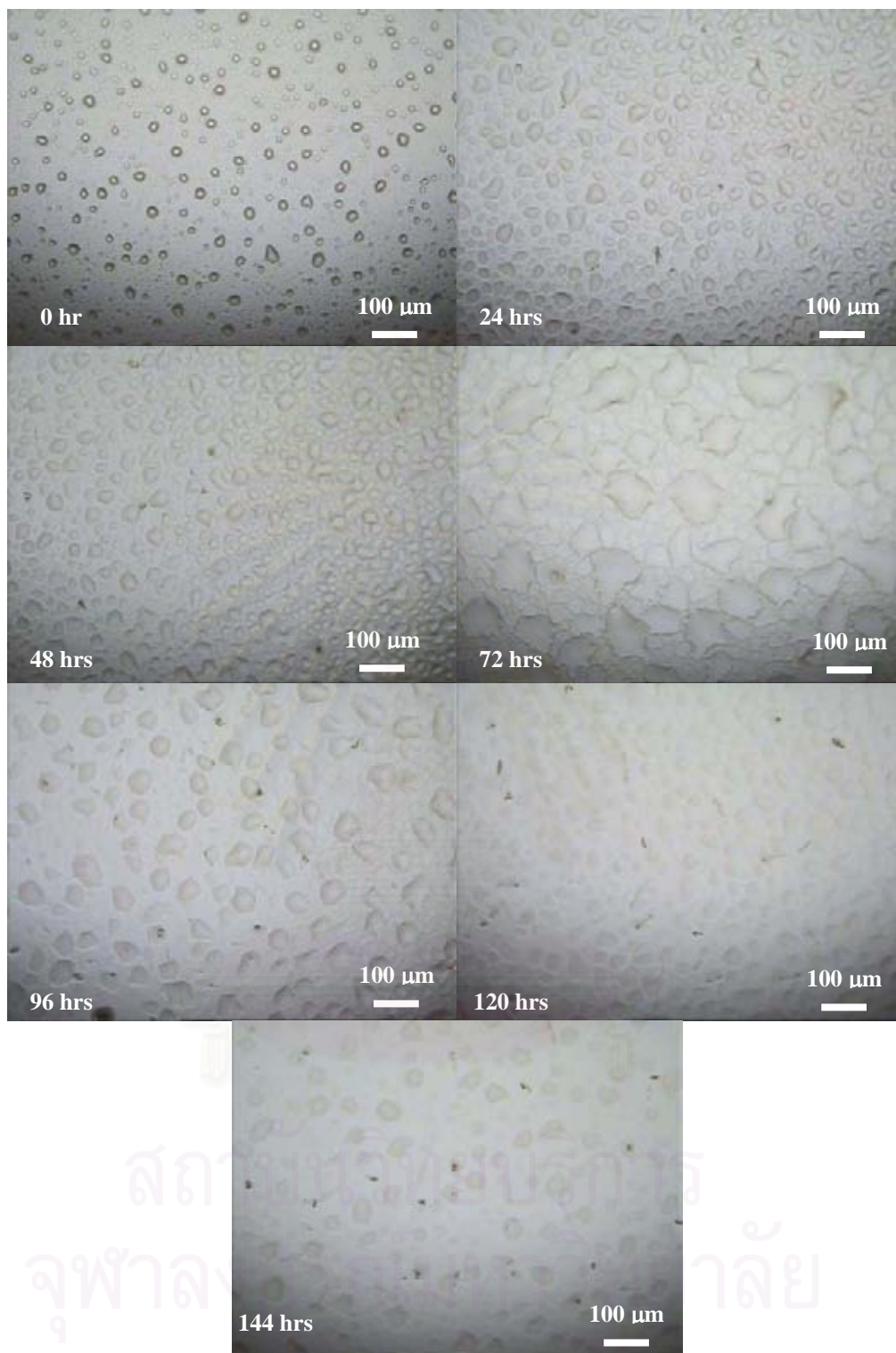
Figure 4.22   Surface characteristic of the NR + TiO$_2$ 0.1 phr films photo-degraded
at different exposure time at the magnification of 20X. (25°C, 7,000
lux)
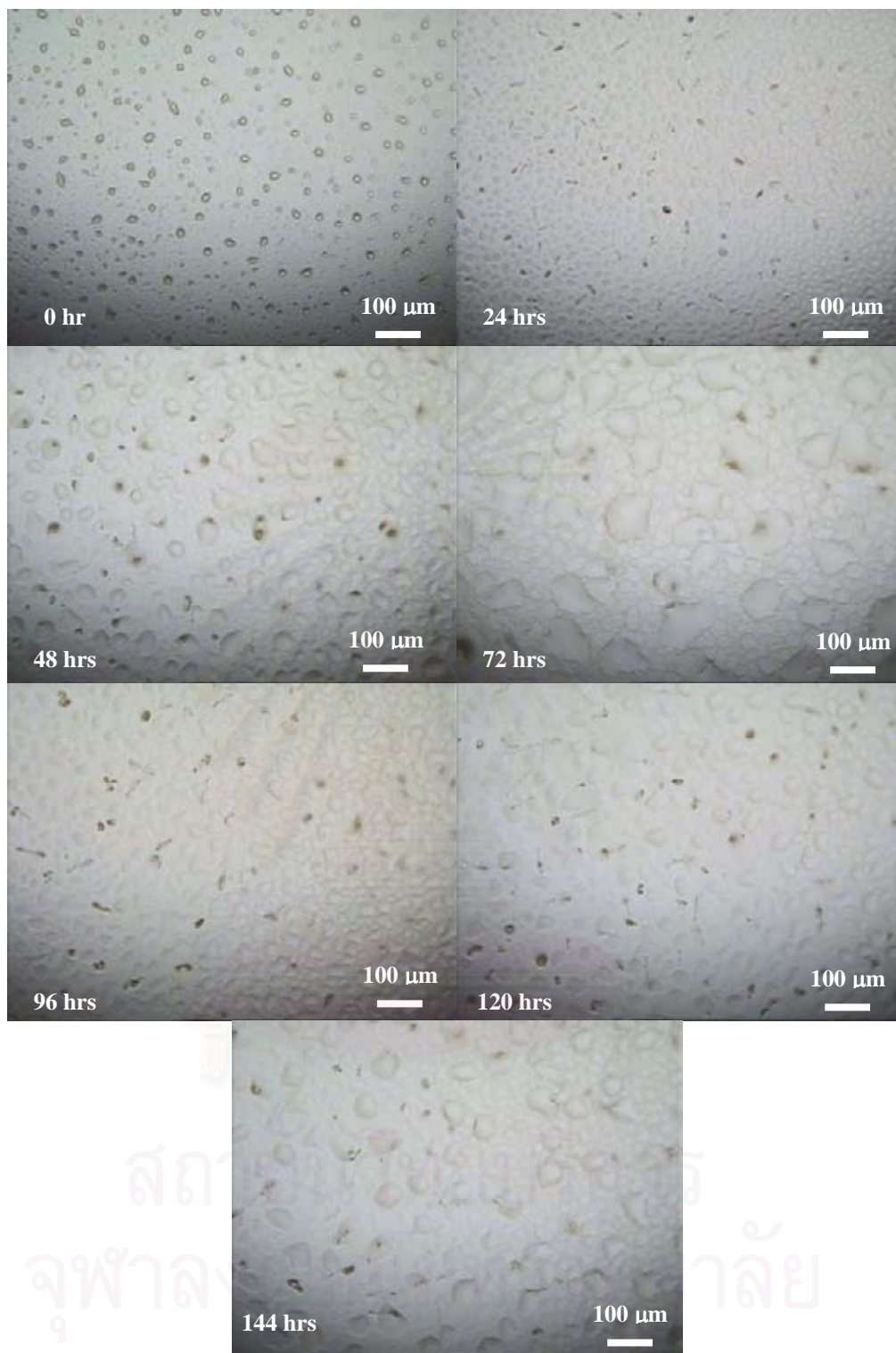
Figure 4.23   Surface characteristic of the NR + $K_2S_2O_8$ 0.1 phr films photo-
degraded at different exposure time at the magnification of 20X.
(25°C, 7,000 lux)

the rubber may show weakness at different locations on the films surface, which can make each location have different surface tensions. Therefore, the shape of the holes on the surface of the NR films may change due to the above reason. The pure NR films have bigger holes when the exposure time was increased. But at 144 hrs of exposure time, it can be noticed that all the holes disappear. The reason is that the NR films surface becomes fluid, which makes the films surface turn to be smoother. At 24 hrs of exposure, the films surface of NR + $K_2S_2O_8$ has quite smaller holes than others. This is probably because $K_2S_2O_8$ can be dissolved in the water, so it can disperse very well in the rubber matrix, and can help degrade the rubber uniformly.

4.4. Viscosity of the natural rubber solution

Viscosity of the rubber solution is one of the important properties of the rubber. It relates to size and shape of the rubber in the solution. From the equations in the topic of solution viscosity in Chapter II, the reduced viscosities (η_{sp}/c) of the pure NR films in toluene are obtained as shown in Figure 4.24. The NR films used in this section have been photo-degraded at the following condition.

Light density (lux)	:	36,000
Temperature (°C)	:	25
Exposure time (hrs)	:	0, 24, 48, 96, 196

From the reduced viscosity in Figure 4.24, the intrinsic viscosities ($[\eta]$) of the NR solution can be obtained by an extrapolation of the experimental values of the reduced viscosity to zero concentration (Table 4.4). From the R^2 values obtained from the graph in Figure 4.24, we can see that the values at the exposure time of 0 and 24 hrs are very low that the intrinsic viscosities obtained at this condition are not reliable. So, only the data at 48, 96, and 196 are quite reliable.

From the intrinsic viscosities obtained, we can plot the intrinsic viscosities versus the *Mw* obtained from the GPC analysis, according to the equation (2.26) or (2.27). From the plots shown in Figure 4.25, it is obvious that the curve obtained is a non-linear curve, and the slope of the curve is negative. As explain in Chapter II, the calibration curve of the viscosity versus *Mw*, such as in Figure 4.25, should be a linear curve, and the slope should be positive. But in this case, the samples that are used are

not the samples that have been carefully fractionated in a small Mw range. And Mw range that is useful for the calibration curve is between 10^4 and 10^6, as we can see from Figure 4.25 that the curve below the Mw of 10^6 tends to have a positive slope. Another reason is that the NR itself has a wide range of Mw, which can affect the viscosity value. Therefore, it is not suitable to use the NR for making a viscosity-Mw calibration curve for a simple Mw analysis.
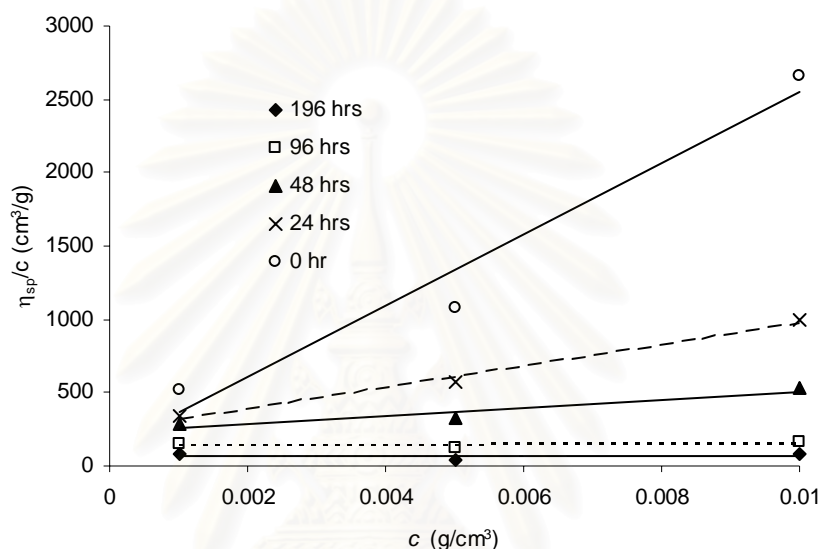
Figure 4.24   Reduced viscosity of pure NR films photo-degraded at different exposure time in toluene at 35°C as a function of concentration.

Table 4.4   Intrinsic viscosities of pure natural rubber at different exposure time in toluene at 35°C.

Exposure time (hrs)	Mw	R^2	$[\eta]$ (cm^3/g)	Huggins constant
0	1,908,649	0.0072	65.37	0.0814
24	1,475,838	0.1340	137.64	0.0847
48	953,822	0.9272	231.61	0.5192
96	384,213	0.9875	247.88	1.1755
196	209,876	0.9576	128.70	14.6041
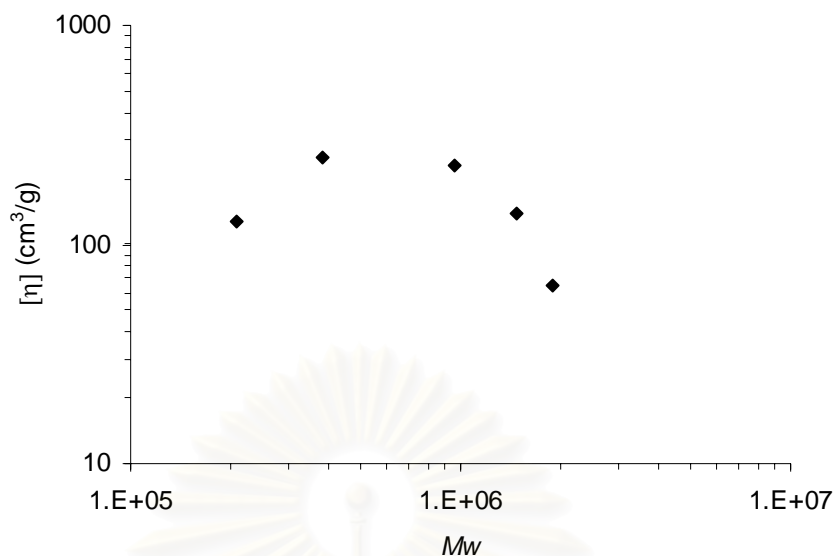
Figure 4.25   Dependence of intrinsic viscosity of natural rubber in toluene at 35°C
on molecular weight.

4.5.   <u>Function groups analysis</u>

The NR films tested at different exposure time were examined by using the
FTIR to study the effect of the photo-degradation on the functional groups, especially
the double bonds, in the NR. The NR films used to analyze are the films that were
photo-degraded at the following condition.

Light density (lux)   :   36,000
Temperature (°C)   :   80
Exposure time (hrs)   :   0, 24, 48, 96, 192

The FTIR spectra of the NR films are shown in Figure 4.26. The peaks that
can be noticed for the changes in the intensity are the peaks at the wave numbers of
1664, 1711, and 1744 cm^{-1}. Refer to Santos's work (2005), for *cis*-polyisoprene, the
wave numbers of 1665, 1715, and 1766 cm^{-1} represent C=C stretching, C=O
stretching of carboxylic acids, and C=O stretching of ketones, respectively. The
positions of the peaks in the author's work are quite close to the wave numbers
referred in Santos's work. Therefore, in the author's work, the peaks at 1664, 1711,

and 1744 cm^{-1} are assumed to be the peaks of C=C stretching, C=O stretching of carboxylic acids, and C=O stretching of ketones, respectively.
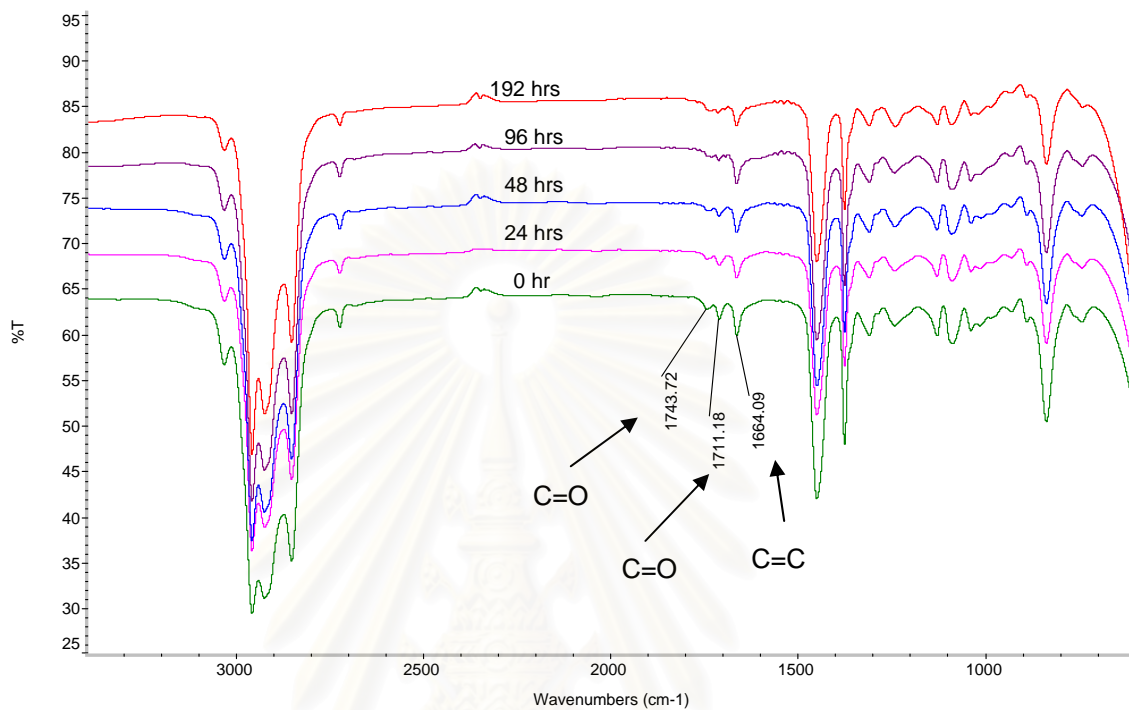
Figure 4.26   FTIR spectra of the natural rubber films photo-degraded at different exposure time.

From Figure 4.26, it can be observed that the intensity of C=C peak decreases a little bit as the exposure time increases. Although the change of the peak intensity is not significant, it is quite consistent to the number of double bonds calculated by using the author's method in that the number of double bonds does not decrease much with the exposure time. According to the *Mw* reduction, the *Mw* of the NR films is reduced as the exposure time increases, and it becomes quite stable at a *Mw* value. It was discussed here that this is probably because the films are too thick that the oxygen molecules cannot penetrate down through the films. This also supports why the intensity of C=C peak does not decrease significantly with the exposure time. For the peaks of C=O, which are expected to be the photo-products (Santos et al., 2005: 34-43), they also do not increase in the intensity significantly with the exposure time, which is consistent to the reasons mentioned above.

4.6.   Moisture content in the natural rubber films

      The pure NR films photo-degraded at 36,000 lux, 80°C, were analyzed for moisture content by drying at 50°C in an oven until their weights did not change.

Table 4.5   Moisture content in the natural rubber films.

Exposure time	Weight (g)			Moisture content
(hrs)	Before drying	After drying	Weight loss	(%)
0	2.0049	1.9994	0.0055	0.27
24	2.0013	1.9970	0.0043	0.22
48	1.9919	1.9878	0.0041	0.21
72	2.0093	2.0042	0.0051	0.25
96	2.3700	2.3645	0.0055	0.23
144	1.9515	1.9464	0.0051	0.26
192	2.0486	2.0432	0.0054	0.26

      From Table 4.5, it can be observed that the moisture content in the NR films is very low, and it does not change with the exposure time. This exhibits that, even though left in the atmosphere, the NR films do not adsorb moisture easily. If we consider the photos of the NR films surface that were taken using the microscope, we can see that the holes on the films surface are shallow. Therefore, the NR films should not be able to adsorb moisture in the atmosphere into their matrices easily.

4.7.   Simulation of the utilization of the natural rubber films at low temperature

      The NR films were used to store the ice, and kept in a freezer at a temperature below 0°C for at least 30 days. After the test, The NR films were still flexible and looked the same as before testing. From the information of the glass transition temperature (T_g), the T_g of poly(*cis*-1,4-isoprene) is -68°C (Allcock et al., 2003: 535). Therefore, NR, which is mainly composed of poly(*cis*-1,4-isoprene) can tolerate low temperature. Above its T_g, NR can be used without loosing its good properties such as flexibility, in which it will not be rigid. So the NR films should be able to be used for a containment of methane hydrate.

Chapter V

Conclusion

From the results of the experiment, it can be concluded that in the photo-degradation process, the weight-average molecular weight of the natural rubber films reduces with time. Light density and temperature have a significant effect on the reduction of the weight-average molecular weight of the natural rubber films. More light density and higher temperature can reduce more weight-average molecular weight of the natural rubber films. In this work, the concentration of catalyst – TiO_2, and peptizer – $K_2S_2O_8$ does not have a significant effect on the reduction of the weight-average molecular weight of the natural rubber films in the photo-degradation process. The concentration of retardant – TiO_2 has a significant effect on the reduction of the weight-average molecular weight of the natural rubber films in the photo-degradation process. More concentration of TiO_2 (> 1 phr) can help reduce the reduction of the weight-average molecular weight of the natural rubber films. For kinetic aspect, the kinetic model for the 1st order reaction with random chain scission

$$\frac{1}{Mw} = \frac{1}{Mw_0} + \frac{kt}{2M_0} \tag{2.7}$$

can be applied to the photo-degradation of the natural rubber films. Moreover, the number of double bonds in the natural rubber films is able to be predicted by using the proposed method of calculation of double bonds in the natural rubber films. Light density and temperature have a significant effect on the reduction of double bonds in the natural rubber films. More light density and higher temperature can reduce more double bonds in the natural rubber films. In this work, the concentration of catalyst – TiO_2, and peptizer – $K_2S_2O_8$ does not have a significant effect on the reduction of double bonds in the natural rubber films in the photo-degradation process. The vulcanizing agent can help reinforce the natural rubber films. In addition, the vulcanization of the natural rubber films can take place simultaneously with the photo-degradation. For a simple weight-average molecular weight analysis, natural rubber is not suitable for making a viscosity-*Mw* calibration curve. And for the application at low temperature, the natural rubber films can be used at a temperature below 0°C without loosing its physical properties.

From the information obtained, it can be seen that the NR films should be able to be applied with the natural gas application. For example, the NR films that were cracked by photo-degradation will become more porous and have more surface area, in which the NR films can adsorb natural gas inside the pores. Further more, because the T_g of NR is low, the NR films should be able to store methane hydrate without loosing their physical properties.

Suggestion

From all the work that has been done here, there are still some aspects that should be further studied. The first one is the thickness of the natural rubber films, which should have a significant effect on the photo-degradation of the films. In this work, it was supposed that because the NR films were too thick, therefore, the catalysts seemed not to have any significant effects on this photo-degradation process. So the thickness of the NR films should be reduced in the further study. The second aspect is the calculation method of the double bonds. There should be more investigation on the reduction of double bonds in the NR films such as by measuring the amount of oxygen used to react with the NR films in the photo-degradation process, and analyze the products obtained using FTIR and NMR, etc., and compare the result with that obtained from using the proposed calculation method.

References

Adam, C., Lacoste, J., and Lemaire, J. Photo-oxidation of elastomeric materials. Part 1 – Photo-oxidation of polybutadienes. Polymer Degradation and Stability 24 (1989) : 185.

Adam, C., Lacoste, J., and Lemaire, J. Photo-oxidation of elastomeric materials. Part IV – Photo-oxidation of 1,2-polybutadienes. Polymer Degradation and Stability 29 (1990) : 305.

Adam, C., Lacoste, J., and Lemaire, J. Photo-oxidation of polyisoprene. Polymer Degradation and Stability 32 (1991) : 51.

Allcock, H.R., Lampe, F.W., and Mark, J.E. Contemporary polymer chemistry. New Jersey : Pearson Education, Inc., 2003.

Andrady, A.L., Hamid, S.H., Hu, X., and Torikai, A. Effects of increased solar ultraviolet radiation on materials. Journal of Photochemistry and Photobiology 46 (1998) : 96.

Arabatzis, I.M., Stergiopoulos, T., Bernard, M.C., Labou, D., Neophytides, S.G., and Falaras, P. Silver-modified titanium dioxide thin films for efficient photodegradation of methyl orange. Applied Catalysis B: Environmental 42 (2003) : 187.

Beauchamp, B. Natural gas hydrates: myths, facts and issues. Comptes Rendus Geoscience 336 (2004) 751-765.

Bhowmick, A.K., Heslop, J., and White, J.R. Photodegradation of thermoplastic elastomeric rubber-polyethylene blends. Journal of Applied Polymer Science 86 (2002) : 2393.

Chapman, P.K., and Haynes, W.E. Power from space and the hydrogen economy. Acta Astronautica 57 (2005) : 372.

Chatti, I., Delahaye, A., Fournaison, L., and Petitet, J.P. Benefits and drawbacks of clathrate hydrates: a review of their areas of interest. Energy Conversion and Management 46 (2005) : 1333.

Cho, S., and Choi, W. Solid-phase photocatalytic degradation of PVC-TiO$_2$ polymer composites. Journal of Photochemistry and Photobiology A: Chemistry 143 (2001) : 221.

Cristopher, R.N., and Forciniti, D. Modeling the ultraviolet photodegradation of rigid polyurethane foams. Industrial Engineering Chemical Research 40 (2001) : 3346.

Fujishima, A., Rao, T.N., and Tryk, D.A. Titanium dioxide photocatalysis. Journal of Photochemistry and Photobiology C: Photochemistry Reviews 1 (2000) : 1-21.

Gijsman, P., Meijers, G., and Vitare, G. Comparison of the UV-degradation chemistry of polypropylene, polyethylene, polyamide 6 and polybutylene terephthalate. Polymer Degradation and Stability 65 (1999) : 433.

Hensel, M., Menting, K.H., Mergenhagen, T., and Umland, H. New insights into the mastication process. Kautschuk Gummi Kunststoffe 57 (2004) : 95.

Kelen, T. Polymer degradation. Newyork : Van Nostrand Reinhold, 1983.

Kubota H., Hariya Y., Kuroda S., and Kondo T. Effect of photoirradiation on potassium persulfate-surface oxidation of low-density polyethylene film. Polymer Degradation and Stability 72 (2001) : 223.

Maillo, C.M., and White, J.R. Preliminary study of stress aided photodegradation of rubber. Plastics, Rubber and Composites 28 (1999) : 277.

Menting, K., Bertrand, J., Hensel, M., and Umland, H. Good processing and good dynamics using a novel zinc free additive – The ultimate way to NR processing? Kautschuk Gummi Kunststoffe 57 (2004) : 48.

Newman, C.R., and Forciniti, D. Modeling the ultraviolet photodegradation of rigid polyurethane foams. Polymer Degradation and Stability 40 (2001) : 3346.

Roubroeks J.P., Andersson R., Mastromauro D.I., Christensen B.E., and Aman P. Molecular weight, structure and shape of oat $(1\rightarrow3),(1\rightarrow4)$-$\beta$-D-glucan fractions obtained by enzymatic degradation with $(1\rightarrow4)$-β-D-glucan 4-glucanohydrolase from *Trichoderma reesei*. Carbohydrate Polymers 46 (2001) : 275.

Sakkas, V.A., Arabatzis, I.M., Konstantinou, I.K., Dimou, A.D., Albanis, T.A., and Falaras, P. Metolachlor photocatalytic degradation using TiO_2 photocatalysts. Applied Catalysis B: Environmental 49 (2004) : 195.

Santos, K.A.M., Suarez, P.A.Z., and Rubim, J.C. Photo-degradation of synthetic and natural polyisoprenes at specific UV radiations. Polymer Degradation and Stability 90 (2005) : 34.

Shang, J., Chai, M., and Zhu, Y. Photocatalytic degradation of polystyrene plastic under fluorescent light. Environmental Science & Tecnology 37 (2003a) : 4494.

Shang, J., Chai, M., and Zhu, Y. Solid-phase photocatalytic degradation of polystyrene plastic with TiO_2 as photocatalyst. Journal of Solid State Chemistry 174 (2003b) : 104.

Tanford, C. Physical chemistry of macromolecules. Newyork : Wiley, 1961.

Turton T.J., and White J.R. Effect of stabilizer and pigment on photo-degradation depth profiles in polypropylene. Polymer Degradation and Stability 74 (2001) : 559.

Wikipedia, the free encyclopedia. Wikipedia: text of the GNU free document license. Boston : Free Software Foundation, Inc., 2002.

Zhang, T., Oyama, T., Horikoshi, S., Zhao, J., Serpone, N., and Hidaka, H. Photocatalytic decomposition of the sodium dodecylbenzene sulfonate surfactant in aqueous titania suspensions exposed to highly concentrated solar radiation and effects of additives. Applied Catalysis B: Environmental 42 (2003) : 13.

APPENDICES

Appendix A

Weight-Average Molecular Weight Data

Table A-1   Weight-average molecular weight data of the 1st experiment in the topic 4.1.1.

Light density (lux)	Exposure time (hrs)	TiO$_2$ (phr)	Average Mw	Max. Mw	Min. Mw
0	0	0	1,256,827	1,275,370	1,244,750
0	0	2	1,246,340	1,266,040	1,208,910
0	24	0	1,417,645	1,518,870	1,337,450
0	24	2	1,317,223	1,341,750	1,295,840
0	48	0	1,066,136	1,189,580	877,029
0	48	2	764,352	1,097,590	569,275
36,000	24	0	895,248	955,443	784,559
36,000	24	2	951,071	1,054,230	708,361
36,000	48	0	427,767	470,109	277,026
36,000	48	2	533,398	650,529	385,515

Table A-2   Weight-average molecular weight data of the 2nd experiment in the topic 4.1.1.

Light density (lux)	Exposure time (hrs)	TiO$_2$ (phr)	Mw
0	0	0.0	1,233,053
0	0	0.5	1,184,887
0	24	0.0	1,243,740
0	24	0.5	1,315,370
0	48	0.0	1,186,010
0	48	0.5	1,271,813
36,000	24	0.0	781,239
36,000	24	0.5	602,727
36,000	48	0.0	196,244
36,000	48	0.5	184,025

Table A-3   Weight-average molecular weight data of the experiment in the topic 4.1.2. (25°C, 36,000 lux).

Exposure time (hrs)	Mw								
	NR + TiO$_2$				NR	NR + K$_2$S$_2$O$_8$			
	1 phr	2 phr	4 phr	8 phr		0.05 phr	0.5 phr	1 phr	2 phr
0	737,496	822,043	958,142	448,303	932,927	865,036	941,389	866,268	542,226
24	165,444	328,810	372,719	352,781	392,470	373,284	304,776	9,904	219,311
48	66,314	156,254	179,066	184,714	100,698	153,951	6,089	97,699	7,542
96	72,059	108,619	90,056	123,017	4,701	70,558	101,143	97,590	91,035
192	215,550	290,139	382,389	561,565	152,256	156,838	128,537	110,411	79,002

Table A-4   Weight-average molecular weight data of the experiment in the topic 4.1.3. (25°C, 36,000 lux).

Exposure time (hrs)	TiO$_2$ concentration in NR (phr)					
	0	0.1	0.2	0.5	0.7	1
0	1,908,649	1,943,106	1,910,890	1,984,274	1,802,730	1,957,032
24	1,475,838	1,307,134	1,244,525	1,276,236	1,242,302	1,200,802
48	953,822	801,742	700,139	821,699	1,084,477	1,223,089
96	384,213	306,340	407,675	440,144	525,304	543,858
192	209,876	209,904	226,010	367,627	392,155	408,550

Exposure time (hrs)	K$_2$S$_2$0$_8$ concentration in NR (phr)					
	0.1	0.2	0.5	0.7	1	1.5
0	1,817,503	1,817,558	1,761,436	1,608,396	1,281,787	1,495,380
24	996,271	903,336	943,371	771,714	634,765	757,356
48	646,262	536,665	515,275	545,246	590,855	428,547
96	307,693	277,112	318,529	354,534	356,245	268,391
192	177,794	178,528	192,754	224,049	258,950	212,498

Table A-5   Weight-average molecular weight data of the experiment in the topic 4.1.4. (25°C, 36,000 lux).

a) NR

Exposure time (hrs)	Mw		
	1	2	Average
0	1,908,649	2,014,739	1,961,694
24	1,475,838	1,110,102	1,292,970
48	953,822	965,131	959,477
72	364,397	456,822	410,610
96	384,213	362,920	373,566
144	250,823	148,156	199,490
192	209,876	145,576	177,726

b) NR + TiO$_2$ 0.1 phr

Exposure time (hrs)	Mw		
	1	2	Average
0	1,943,106	1,771,786	1,857,446
24	1,307,134	1,328,760	1,317,947
48	801,742	727,655	764,699
72	344,039	493,463	418,751
96	306,340	442,903	374,621
144	195,218	194,283	194,751
192	209,904	196,298	203,101

c)   NR + $K_2S_2O_8$ 0.1 phr

Exposure time (hrs)	Mw		
	1	2	Average
0	1,817,503	1,764,500	1,791,001
24	996,271	1,236,792	1,116,532
48	646,262	920,578	783,420
72	342,157	438,037	390,097
96	307,693	298,752	303,222
144	184,534	185,171	184,853
192	177,794	152,784	165,289

Table A-5   Weight-average molecular weight data of the experiment in the topic 4.1.4. (80°C, 36,000 lux).

Exposure time (hrs)	Mw		
	NR	NR + TiO_2 0.1 phr	NR + $K_2S_2O_8$ 0.1 phr
0	1,703,425	1,649,092	1,801,994
24	611,273	673,546	763,187
48	373,823	513,919	414,844
72	332,508	260,666	278,722
96	234,133	236,644	254,941
144	201,530	197,818	210,796
192	182,730	183,795	184,476

Table A-6   Weight-average molecular weight data of the experiment in the topic 4.1.5. (25°C, 7,000 lux).

Exposure time (hrs)	Mw		
	NR	NR + TiO_2 0.1 phr	NR + $K_2S_2O_8$ 0.1 phr
0	983,396	990,416	747,605
24	845,655	921,170	849,826
48	801,240	792,607	791,281
72	853,640	856,623	815,705
96	907,278	878,095	706,514
120	755,323	566,568	626,450
144	433,277	464,880	609,013
192	-	306,776	379,205

Appendix B

2^k Experimental Design Data

Below is the sample of calculation of 2^k experimental design in the topic 4.1.1.

Table B-1   The data of the 1st experiment.

		Factor Level	
		Low (-1)	High (+1)
TiO$_2$ (phr)	A	0	2
Light density (lux)	B	0	36,000
Time (hrs)	C	24	48

Table B-2 2^3 Factorial design.

					Mw			
Run no.	A	B	C	Run label	Replicate 1	Replicate 2	Sum	Average
1	-1	-1	-1	(1)	1,356,970	1,478,320	2,835,290	1,417,645
2	1	-1	-1	a	1,320,370	1,314,077	2,634,447	1,317,223
3	-1	1	-1	b	946,478	844,017	1,790,496	895,248
4	1	1	-1	ab	897,344	1,004,798	1,902,142	951,071
5	-1	-1	1	c	1,112,143	1,020,129	2,132,272	1,066,136
6	1	-1	1	ac	911,627	617,076	1,528,703	764,352
7	-1	1	1	bc	396,103	459,430	855,533	427,767
8	1	1	1	abc	435,319	631,478	1,066,797	533,398

Table B-3   Contrast coefficients used in estimating effects.

Run label	A	B	AB	C	AC	BC	ABC
(1)	-1	-1	1	-1	1	1	-1
a	1	-1	-1	-1	-1	1	1
b	-1	1	-1	-1	1	-1	1
ab	1	1	1	-1	-1	-1	-1
c	-1	-1	1	1	-1	-1	1
ac	1	-1	-1	1	1	-1	-1
bc	-1	1	-1	1	-1	1	-1
abc	1	1	1	1	1	1	1

Table B-4   Contrast used in estimating effects.

Run label	A	B	AB	C	AC	BC	ABC
(1)	-2835290	-2835290	2835290	-2835290	2835290	2835290	-2835290
a	2634447	-2634447	-2634447	-2634447	-2634447	2634447	2634447
b	-1790496	1790496	-1790496	-1790496	1790496	-1790496	1790496
ab	1902142	1902142	1902142	-1902142	-1902142	-1902142	-1902142
c	-2132272	-2132272	2132272	2132272	-2132272	-2132272	2132272
ac	1528703	-1528703	-1528703	1528703	1528703	-1528703	-1528703
bc	-855533	855533	-855533	855533	-855533	855533	-855533
abc	1066797	1066797	1066797	1066797	1066797	1066797	1066797
Sum	-481502	-3515745	1127322	-3579069	-303108	38454	502343

Table B-5   Effect estimates summary.

Model Term	Contrast	Effect Estimate	Sum of Squares	Percent Contribution
A	-481502	-60187.79	1.45E+10	0.86
B	-3515745	-439468.13	7.73E+11	45.75
AB	1127322	140915.21	7.94E+10	4.70
C	-3579069	-447383.63	8.01E+11	47.41
AC	-303108	-37888.46	5.74E+09	0.34
BC	38454	4806.71	9.24E+07	0.01
ABC	502343	62792.88	1.58E+10	0.93

Table B-6   Effect estimates for the normal probability plot.

j	$\frac{100*(j-0.5)}{n}$	Effect Estimate
1	7.14	-447384
2	21.43	-439468
3	35.71	-60188
4	50.00	-37888
5	64.29	4807
6	78.57	62793
7	92.86	140915

Table B-7   Analysis of variance.

Source of Variation	Sum of Squares	Degree of Freedom	Mean Square	F_0	P-Value
B	7.73E+11	1	7.73E+11	86.93	4.03E-07
C	8.01E+11	1	8.01E+11	90.09	3.28E-07
Error	1.16E+11	13	8.89E+09		
Total	1.69E+12	15			

Table B-8   Residuals.

A	B	C	Mw	Average	Residual
0	0	24	1356970	1417645	-60675
0	0	24	1478320	1417645	60675
2	0	24	1320370	1317223	3147
2	0	24	1314077	1317223	-3147
0	100	24	946478	895248	51231
0	100	24	844017	895248	-51231
2	100	24	897344	951071	-53727
2	100	24	1004798	951071	53727
0	0	48	1112143	1066136	46007
0	0	48	1020129	1066136	-46007
2	0	48	911627	764352	147275
2	0	48	617076	764352	-147275
0	100	48	396103	427767	-31663
0	100	48	459430	427767	31663
2	100	48	435319	533398	-98079
2	100	48	631478	533398	98079

Table B-9   Data for residuals plot.

Residual	j	(j-0.5)*100/n
-147275	1	3.13
-98079	2	9.38
-60675	3	15.63
-53727	4	21.88
-51231	5	28.13
-46007	6	34.38
-31663	7	40.63
-3147	8	46.88
3147	9	53.13
31663	10	59.38
46007	11	65.63
51231	12	71.88
53727	13	78.13
60675	14	84.38
98079	15	90.63
147275	16	96.88

Appendix C

Sample of Calculation of Double Bonds
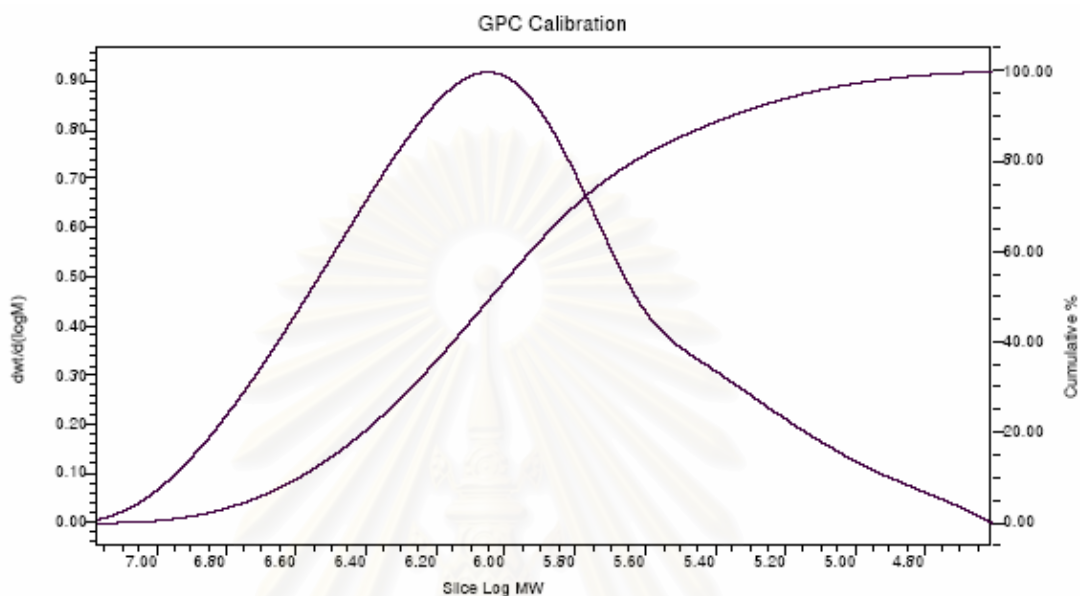
in the Natural Rubber Films

Figure C-1   GPC distribution curve of the NR film at the degradation time of 0 hr
of the experiment in the topic 4.1.4.

Table C-1   Molecular weight distribution data of the NR film at the degradation
time of 0 hr of the experiment in the topic 4.1.4.

Cumulative %	Slice Mw (Daltons)	Slice Area	Cumulative %	Slice Mw (Daltons)	Slice Area
1	8,946,463	4,356	19	2,683,969	25,878
2	7,478,468	6,876	20	2,588,915	26,532
3	6,590,623	8,911	21	2,499,639	27,177
4	5,955,095	10,660	22	2,415,590	27,795
5	5,461,709	12,204	23	2,336,255	28,375
6	5,060,794	13,627	24	2,261,232	28,952
7	4,724,663	14,925	25	2,190,144	29,479
8	4,436,266	16,131	26	2,122,650	30,001
9	4,184,771	17,262	27	2,058,448	30,485
10	3,962,286	18,329	28	1,997,275	30,945
11	3,763,661	19,328	29	1,938,919	31,397
12	3,584,575	20,294	30	1,883,155	31,810
13	3,422,086	21,203	31	1,829,788	32,203
14	3,273,504	22,059	32	1,778,651	32,576
15	3,137,024	22,904	33	1,729,597	32,923
16	3,011,037	23,685	34	1,682,467	33,237
17	2,894,192	24,439	35	1,637,154	33,546
18	2,785,456	25,166	36	1,593,546	33,834

Cumulative %	Slice Mw (Daltons)	Slice Area	Cumulative %	Slice Mw (Daltons)	Slice Area
37	1,551,531	34,095	69	666,934	26,728
38	1,511,016	34,338	70	646,184	25,932
39	1,471,890	34,538	71	625,519	25,095
40	1,434,083	34,735	72	604,912	24,219
41	1,397,510	34,890	73	584,325	23,305
42	1,362,092	35,022	74	563,726	22,362
43	1,327,768	35,128	75	543,098	21,381
44	1,294,476	35,216	76	522,380	20,364
45	1,262,157	35,269	77	501,551	19,334
46	1,230,746	35,291	78	480,581	18,279
47	1,200,197	35,288	79	459,441	17,231
48	1,170,454	35,246	80	438,152	16,213
49	1,141,474	35,177	81	416,728	15,222
50	1,113,211	35,081	82	395,226	14,301
51	1,085,628	34,961	83	373,759	13,479
52	1,058,690	34,805	84	352,452	12,729
53	1,032,355	34,618	85	331,450	12,062
54	1,006,587	34,399	86	310,859	11,451
55	981,350	34,135	87	290,766	10,870
56	956,603	33,827	88	271,196	10,297
57	932,318	33,503	89	252,149	9,702
58	908,466	33,135	90	233,561	9,082
59	885,023	32,736	91	215,393	8,441
60	861,956	32,303	92	197,543	7,726
61	839,240	31,836	93	179,934	7,016
62	816,852	31,323	94	162,506	6,261
63	794,755	30,780	95	145,160	5,468
64	772,929	30,200	96	127,748	4,647
65	751,352	29,590	97	110,033	3,772
66	729,999	28,929	98	91,628	2,847
67	708,820	28,227	99	71,721	1,877
68	687,809	27,491	100	40,993	18

The calculation is started by slicing the GPC distribution curve into 100 pieces, in which each piece represents the weight (Wt) of NR having one Mw, and is done on the basis of 1 kg of NR, the number of molecules (n) of NR in each fraction (x) at time t (0 hr) is then calculated from

$$n_{x,t} = \frac{Wt_{x,t}}{Mw_{x,t}} \times 6.02 \times 10^{23} \qquad (2.8)$$

where $Wt_{x,t}$ is the Wt of NR in each fraction at time t, and $Mw_{x,t}$ is the Mw of NR in each fraction at time t. The total number of molecules or the molecular chains of NR at time t ($n_{total,t}$) is the summation of the number of molecules of NR in each fraction.

$$n_{total,t} = \sum_{x=1}^{100} n_{x,t} \qquad (2.9)$$

Table C-2   Number of molecules and weight fraction of the natural rubber film at the degradation time of 0 hr of the experiment in the topic 4.1.4.

Cumulative %	No. of molecules	Weight (g)	Cumulative %	No. of molecules	Weight (g)
1	1.2508E+17	1.86	50	8.0958E+18	14.97
2	2.3620E+17	2.93	51	8.2731E+18	14.92
3	3.4735E+17	3.80	52	8.4457E+18	14.85
4	4.5987E+17	4.55	53	8.6146E+18	14.77
5	5.7403E+17	5.21	54	8.7793E+18	14.68
6	6.9174E+17	5.82	55	8.9359E+18	14.57
7	8.1153E+17	6.37	56	9.0844E+18	14.44
8	9.3413E+17	6.88	57	9.2317E+18	14.30
9	1.0597E+18	7.37	58	9.3700E+18	14.14
10	1.1884E+18	7.82	59	9.5024E+18	13.97
11	1.3193E+18	8.25	60	9.6277E+18	13.79
12	1.4544E+18	8.66	61	9.7453E+18	13.59
13	1.5917E+18	9.05	62	9.8511E+18	13.37
14	1.7312E+18	9.41	63	9.9494E+18	13.14
15	1.8757E+18	9.77	64	1.0038E+19	12.89
16	2.0208E+18	10.11	65	1.0117E+19	12.63
17	2.1693E+18	10.43	66	1.0181E+19	12.35
18	2.3210E+18	10.74	67	1.0230E+19	12.05
19	2.4769E+18	11.04	68	1.0268E+19	11.73
20	2.6328E+18	11.32	69	1.0295E+19	11.41
21	2.7931E+18	11.60	70	1.0310E+19	11.07
22	2.9560E+18	11.86	71	1.0306E+19	10.71
23	3.1202E+18	12.11	72	1.0286E+19	10.34
24	3.2893E+18	12.36	73	1.0246E+19	9.95
25	3.4578E+18	12.58	74	1.0191E+19	9.54
26	3.6310E+18	12.80	75	1.0114E+19	9.12
27	3.8046E+18	13.01	76	1.0015E+19	8.69
28	3.9803E+18	13.21	77	9.9031E+18	8.25
29	4.1600E+18	13.40	78	9.7712E+18	7.80
30	4.3395E+18	13.57	79	9.6348E+18	7.35
31	4.5213E+18	13.74	80	9.5061E+18	6.92
32	4.7051E+18	13.90	81	9.3839E+18	6.50
33	4.8901E+18	14.05	82	9.2958E+18	6.10
34	5.0750E+18	14.18	83	9.2647E+18	5.75
35	5.2640E+18	14.32	84	9.2781E+18	5.43
36	5.4545E+18	14.44	85	9.3490E+18	5.15
37	5.6454E+18	14.55	86	9.4633E+18	4.89
38	5.8381E+18	14.65	87	9.6039E+18	4.64
39	6.0282E+18	14.74	88	9.7542E+18	4.39
40	6.2224E+18	14.82	89	9.8848E+18	4.14
41	6.4137E+18	14.89	90	9.9895E+18	3.88
42	6.6054E+18	14.95	91	1.0068E+19	3.60
43	6.7966E+18	14.99	92	1.0047E+19	3.30
44	6.9889E+18	15.03	93	1.0017E+19	2.99
45	7.1787E+18	15.05	94	9.8978E+18	2.67
46	7.3665E+18	15.06	95	9.6771E+18	2.33
47	7.5533E+18	15.06	96	9.3451E+18	1.98
48	7.7360E+18	15.04	97	8.8067E+18	1.61
49	7.9169E+18	15.01	98	7.9822E+18	1.21

Cumulative %	No. of molecules	Weight (g)
99	6.7233E+18	0.80
100	1.1280E+17	0.01
Sum	6.5662E+20	1,000.00

From Table C-2, $n_{total,0\ hr} = 6.5662 \times 10^{20}$.

The broken double bonds at time t (B_t) has a relationship as followed.

$$B_t = n_{total,t} \tag{2.11}$$

Suppose that an ideal NR has only one long polyisoprene chain. Each isoprene unit contains one double bond. Therefore, the number of double bonds in the ideal NR (D_{ideal}) is equal to the number of isoprene unit, which can be calculated as followed:

$$D_{ideal} = \frac{Wt_{NR}}{M_0} \times 6.02 \times 10^{23} \tag{2.12}$$

where Wt_{NR} is the weight of NR, and M_0 is the Mw of an isoprene unit, which is equal to 68. Therefore we can get

$$D_{ideal} = \frac{1,000}{68} \times 6.02 \times 10^{23} = 8.8529 \times 10^{24}$$

Finally, we can obtain the number of double bonds in NR at time t (D_t) from

$$D_t = D_{ideal} - B_t \tag{2.13}$$

As a result, we get

$$D_{0hr} = (8.8529 \times 10^{24}) - 6.5662 \times 10^{20} = 8.8523 \times 10^{24}$$

Appendix D

Data of Natural Rubber Solution Viscosity Measurement

Table D-1   Flow time of the solution having different concentration of the natural rubber films photo-degraded at different exposure time. (25°C, 36,000 lux).

C (g/cm^3)	Flow time (sec)				
	196 hrs	96 hrs	48 hrs	24 hrs	0 hr
0.000	20.77	20.77	20.77	20.77	20.77
0.001	22.38	23.91	26.63	27.91	31.52
0.005	25.53	33.70	55.07	79.62	132.27
0.010	37.03	54.65	130.46	226.18	574.34

Table D-2   Relative viscosities of the solution having different concentration of the natural rubber films photo-degraded at different exposure time. (25°C, 36,000 lux).

c (g/cm^3)	η_r				
	196 hrs	96 hrs	48 hrs	24 hrs	0 hr
0.000	1.0000	1.0000	1.0000	1.0000	1.0000
0.001	1.0775	1.1510	1.2820	1.3436	1.5176
0.005	1.2293	1.6224	2.6516	3.8336	6.3682
0.010	1.7829	2.6310	6.2812	10.8896	27.6525

Table D-3   Reduced viscosities of the solution having different concentration of the natural rubber films photo-degraded at different exposure time. (25°C, 36,000 lux).

c (g/cm^3)	η_{sp}/c (cm^3/g)				
	196 hrs	96 hrs	48 hrs	24 hrs	0 hr
0.000	-	-	-	-	-
0.001	78	151	282	344	518
0.005	46	124	330	567	1074
0.010	78	163	528	989	2665

Appendix E

Data of Tensile Strength Analysis

Sample type

A	NR
B	NR + $K_2S_2O_8$ 0.1 phr
C	NR + vulcanizing agent
D	NR + vulcanizing agent + $K_2S_2O_8$ 0.1 phr

Table E-1   Tensile strength data of the natural rubber films photo-degraded at different exposure time. (Tensile stress point = 300) (80°C, 36,000 lux).

Sample type	Sample reference	Thickness (mm)	Tensile strength (MPa)	Ultimate elongation	Tensile stress (MPa)
A 0 hr	1	0.662	1.5612	999	0.5123
	2	0.635	1.4995	1035	0.4771
	3	0.603	-	-	0.5550
	4	0.695	1.8779	1115	0.5275
	5	0.560	-	-	0.3765
B 0 hr	1	0.607	-	-	0.5335
	2	0.602	1.9695	1070	0.5015
	3	0.557	-	-	0.4167
	4	0.587	-	-	0.4439
	5	0.628	2.1306	1061	0.5226
C 0 hr	1	0.653	13.3746	955	1.1324
	2	0.433	8.0652	759	1.2035
	3	0.617	13.5668	870	1.1917
	4	0.582	15.6445	950	1.0691
	5	0.625	15.1216	913	1.1282
D 0 hr	1	0.676	13.4742	983	1.1169
	2	0.622	12.4631	842	1.2469
	3	0.570	14.5628	933	1.0664
	4	0.558	8.1749	1309	1.0984
	5	0.667	13.6106	855	1.2145
C 72 hrs	1	0.492	2.8393	471	1.7396
	2	0.680	4.3518	477	2.3317
	3	0.650	8.6289	570	2.1285
	4	0.602	6.9762	590	1.9125
	5	0.713	10.5303	620	2.0749
	6	0.698	7.1496	500	2.3662
D 72 hrs	1	0.560	1.6717	274	-
	2	0.580	4.4004	493	2.0995
	3	0.590	3.7814	497	1.9565
	4	0.590	3.5729	515	1.6815
	5	0.590	3.6931	560	1.5369

Sample type	Sample reference	Thickness (mm)	Tensile strength (MPa)	Ultimate elongation	Tensile stress (MPa)
C 72 hrs simultaneous	1	0.527	4.3556	570	1.6330
	2	0.527	6.1586	628	1.6185
	3	0.528	6.5375	661	1.5893
	4	0.527	7.5831	695	1.6407
	5	0.530	6.9378	632	1.6365
D 72 hrs simultaneous	1	0.500	6.5226	663	1.6270
	2	0.503	4.0273	702	1.1759
	3	0.533	5.5120	683	1.3860
	4	0.530	2.8532	425	1.8831
	5	0.492	2.8790	487	1.7515
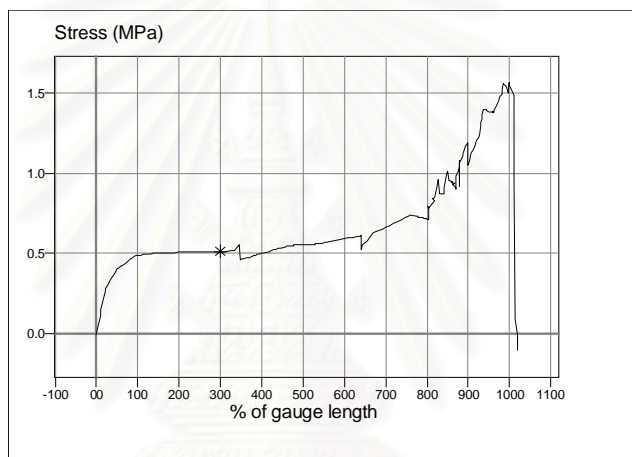
Figure E-1   Tensile stress diagram of sample A, 0 hr.
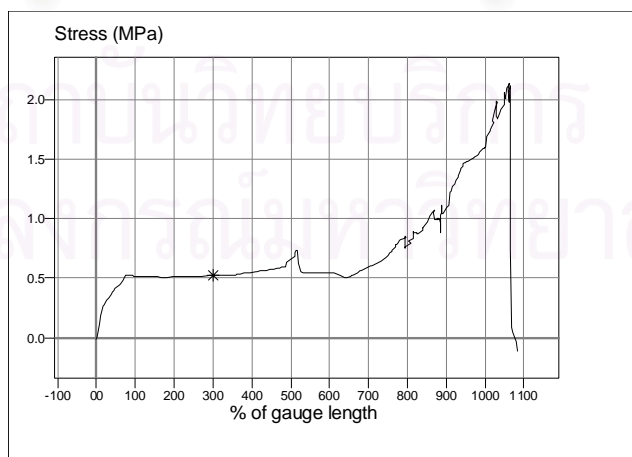
Figure E-2   Tensile stress diagram of sample B, 0 hr.
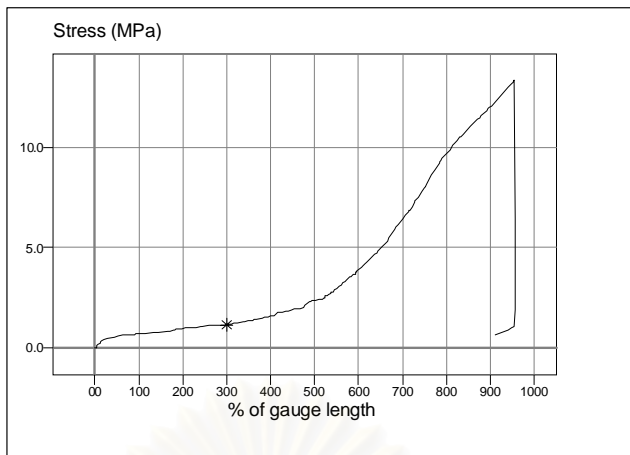
Figure E-3   Tensile stress diagram of sample C, 0 hr.
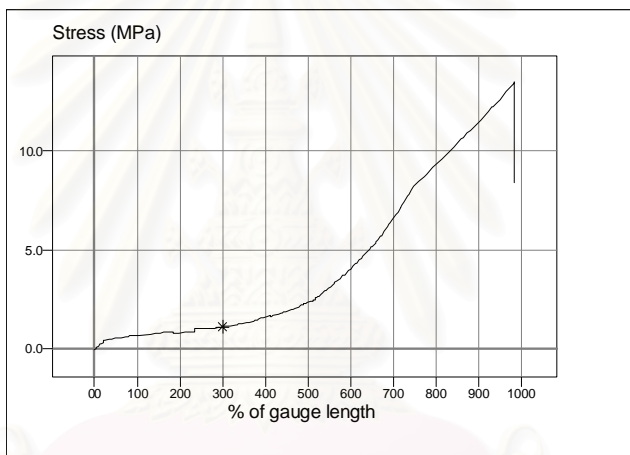
Figure E-4   Tensile stress diagram of sample D, 0 hr.
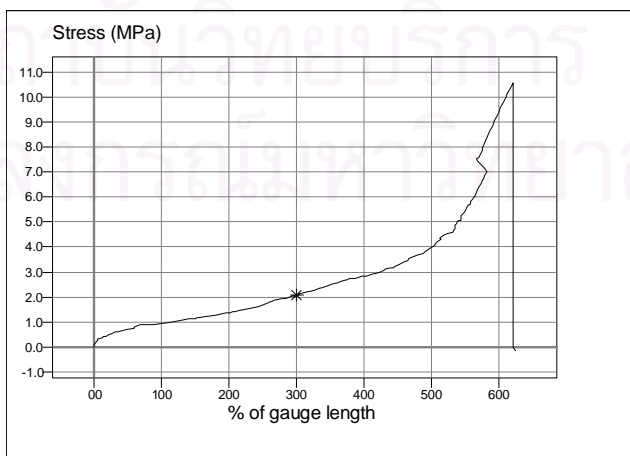

Figure E-5   Tensile stress diagram of sample C, 72 hr.
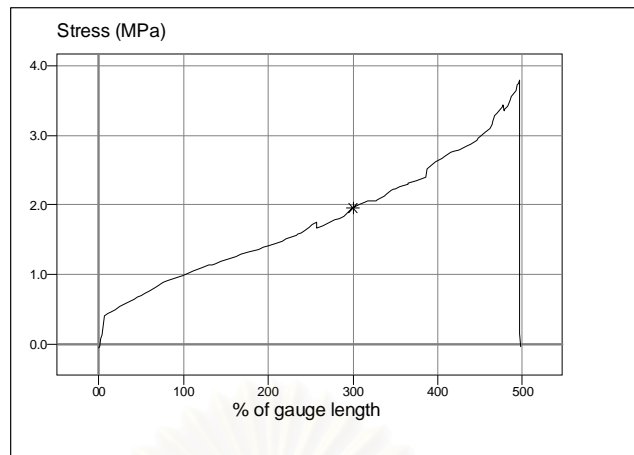
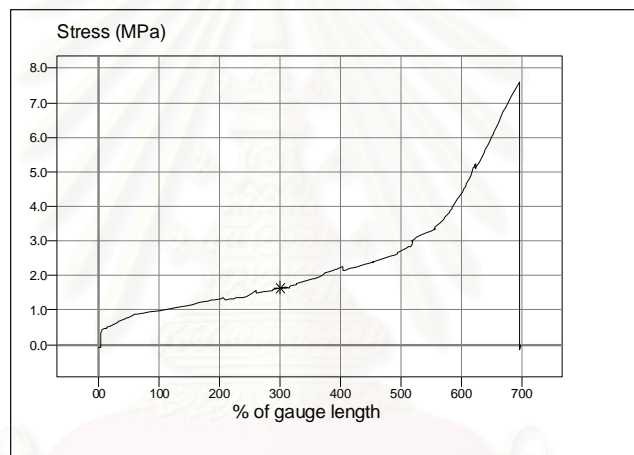Figure E-6   Tensile stress diagram of sample D, 72 hr.

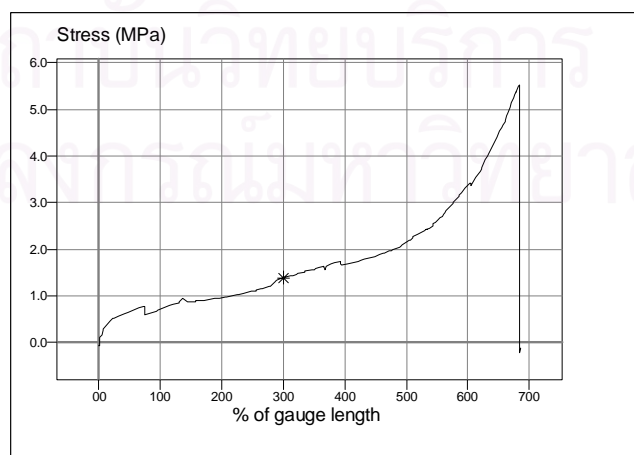Figure E-7   Tensile stress diagram of sample C, 72 hr, simultaneous.

Figure E-8   Tensile stress diagram of sample D, 72 hr, simultaneous.

Appendix F

Gas Permeability of Natural Rubber Films

Table F-1   Frazier permeability of the natural rubber films

No.	Frazier permeability ($ft^3.min^{-1}.ft^{-2}$ per 0.5 inches of water)
1	0.0109
2	0.0119
3	0.0046
4	0.0061
Average	0.0084

Biography

The author, Miss Wannipha Amatyakul, was born on March 8, 1976, in Bangkok. She studied Chemical Technology in the Chemical Technology Department, Faculty of Science, Chulalongkorn University for bachelor and master degrees, in which she graduated in 1997 and 2001, respectively. She starts her doctoral program in 2002, in the same field of study. At present, she is working as the Development Supervisor at Thai Auromex Co., Ltd.